



Stainless steel slags and the use of ChemApp

Bart Blanpain

**Dirk Durinck, Sander Arnout, P. Tom Jones, Muxing Guo, Frederik
Verhaeghe, Patrick Wollants**

Thermodynamics in Materials Engineering

Dept. Metaalkunde en Toegepaste Materiaalkunde

Katholieke Universiteit Leuven, Belgium

GTT – 5 June 2008



Outline

- Introduction
- EAF process in stainless steel production
- Slag stabilisation and microstructure calculation



Katholieke Universiteit Leuven









Thermodynamics in Materials Engineering Research Group

Department

of

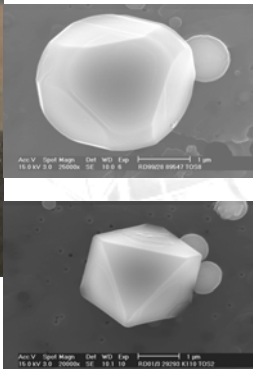
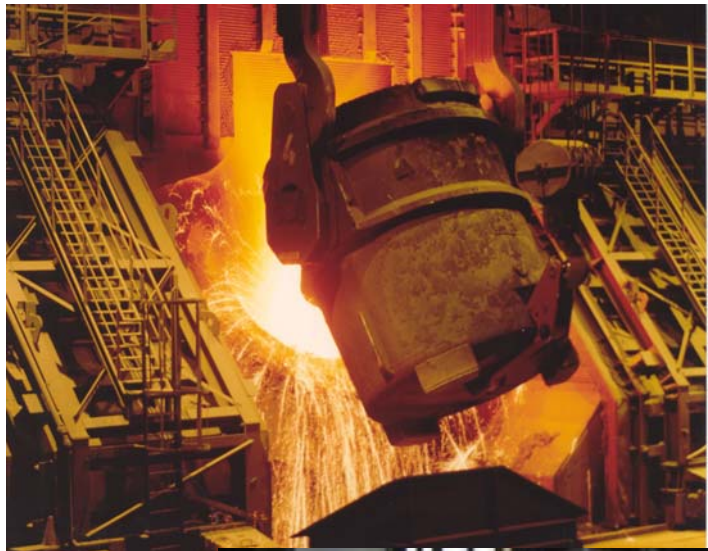
Metallurgy and Materials Engineering





I. Pyrometallurgical processing

- Vessel integrity
- Slag practice and properties
- Steel cleanliness
- Modelling



Acq. V.: 1.0 kV; Spot Mag.: 3.0; Det: WD; Exp.: 10.0 s; RDIMAG: 400-CL-73911-61; 1 μm

Centre for high temperature processes, metallurgy and refractory materials

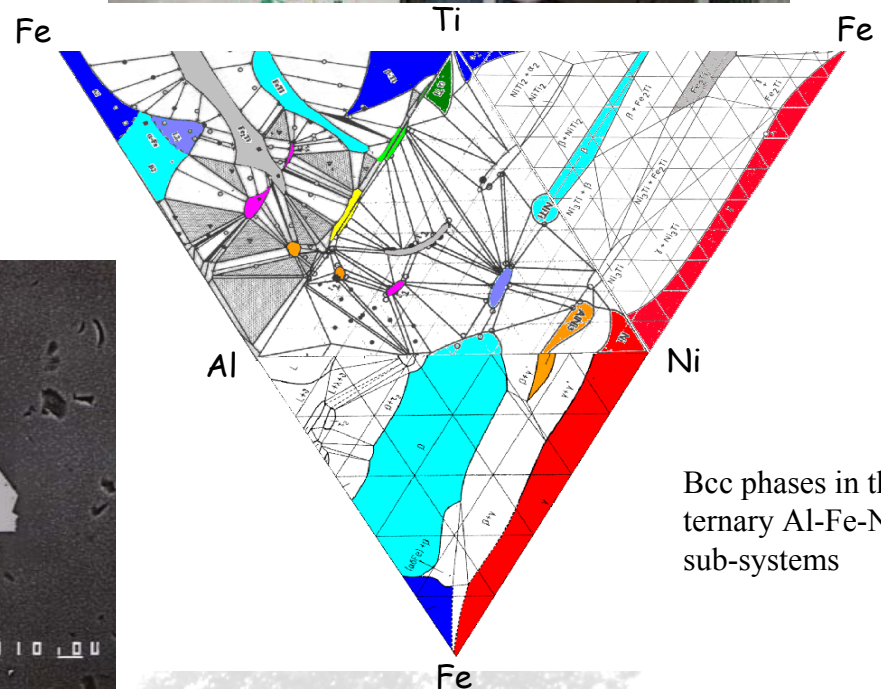
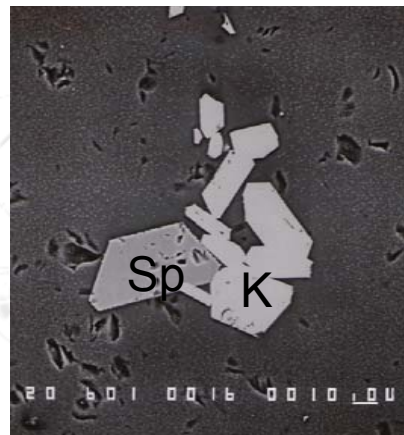


- Cooperation with industrial partners active in high temperature metals processing:
ArcelorMittal, Heraeus Electro-Nite and Umicore
- Fly wheel function for intense collaboration through substantial research projects and doctoral research programs



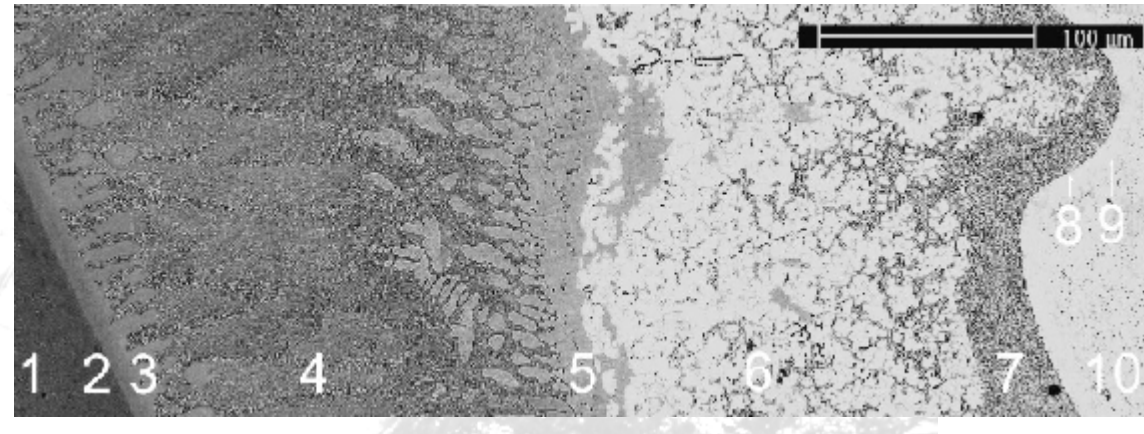
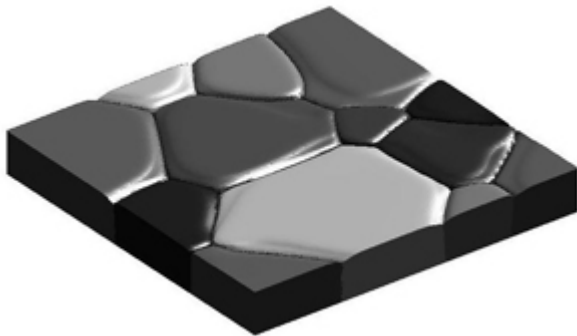
II. Phase relations in materials systems

- ❑ Determination and optimisation of phase diagrams in metallic systems
 - ❑ Phase relations in slag systems
 - ❑ Thermodynamics of nanomaterials systems



III. Microstructure evolution modelling

- Grain growth
- Lead-free solder systems
- Dissolution of ferro-alloys in liquid steel
- Solidification of slags





Stainless steel slags



Steel production sites in Belgium



Steel production sites in Belgium



Stainless steel slags

□ General

- By-product/waste of stainless steel production
- Metallurgical functions:
 - * Oxidation shielding
 - * Impurity removal
 - * Thermal insulation

□ Amounts

- Slag-to-steel ratio: 275 kg slag / 1000 kg steel
- Global stainless steel production: 25 Mt steel
(source: ISSF, IISI)

→ ~ 7 Mt stainless steel slag / year

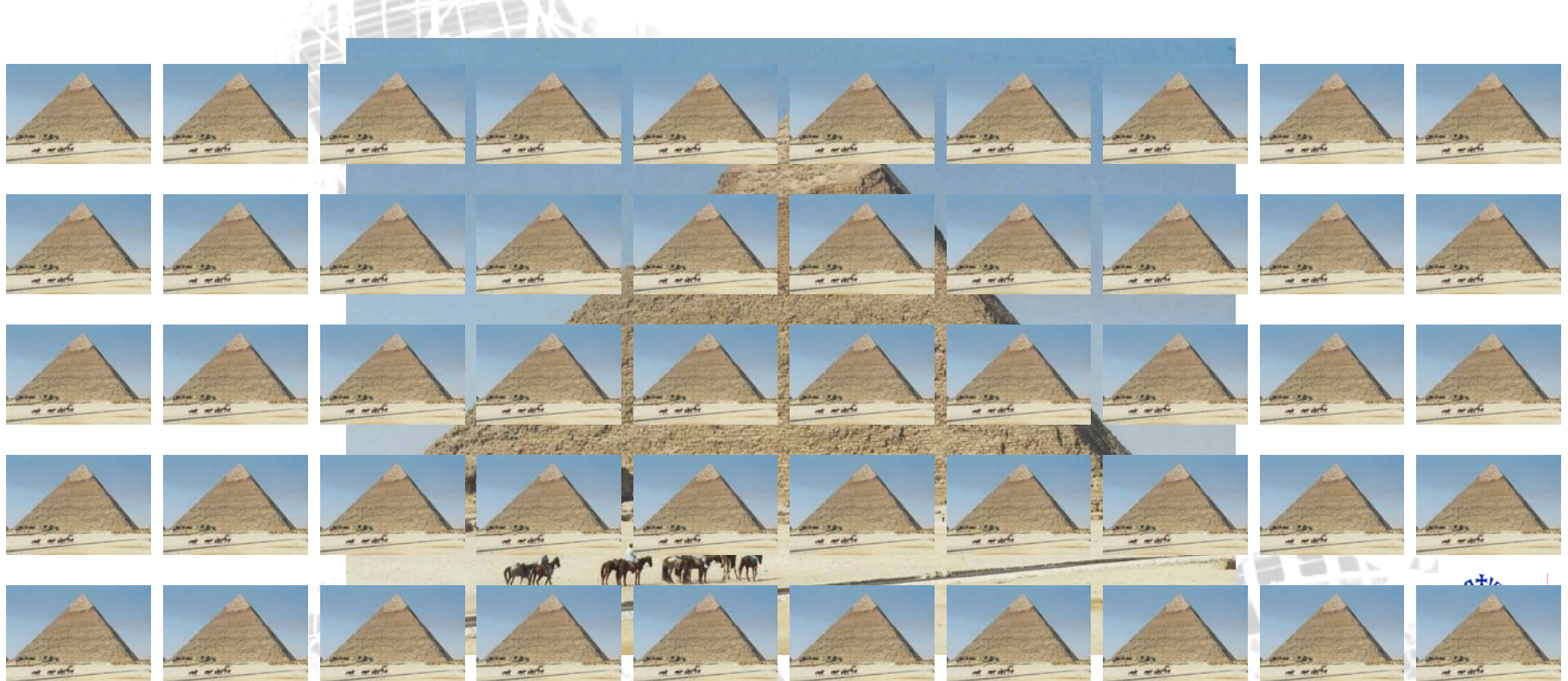


Assumptions: density = 2.5 ton/m³, Gizeh pyramid dimensions = 230m.230m.137m

World steel production: $\sim 1.25 \cdot 10^9$ tons

Slag/steel ratio: 1/3 \sim 1/4

World iron and steel slag production: $\sim 350 \cdot 10^6$ tons

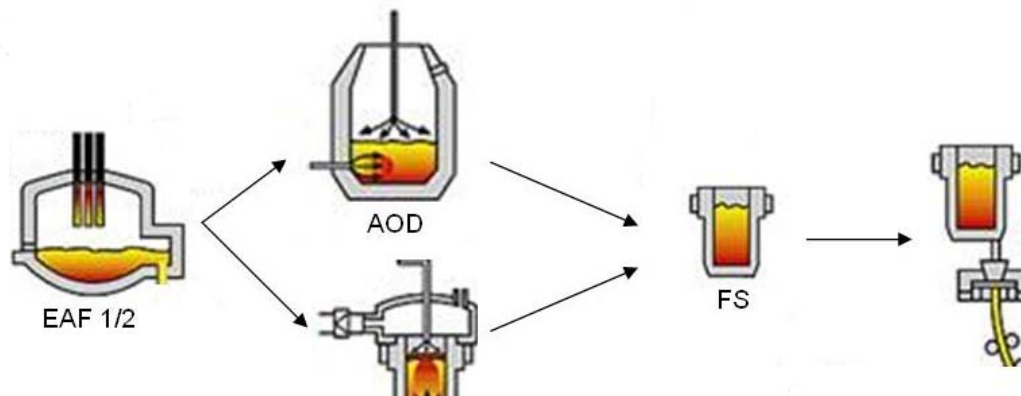


Assumptions: density = 2.5 ton/m³, Gizeh pyramid dimensions = 230m.230m.137m

Stainless steel production

- 3-step process (before casting)

- EAF: scrap melting
- AOD/VOD: de-C and de-S
- Ladle refining: de-S



EAF slag

125 kg/ton steel

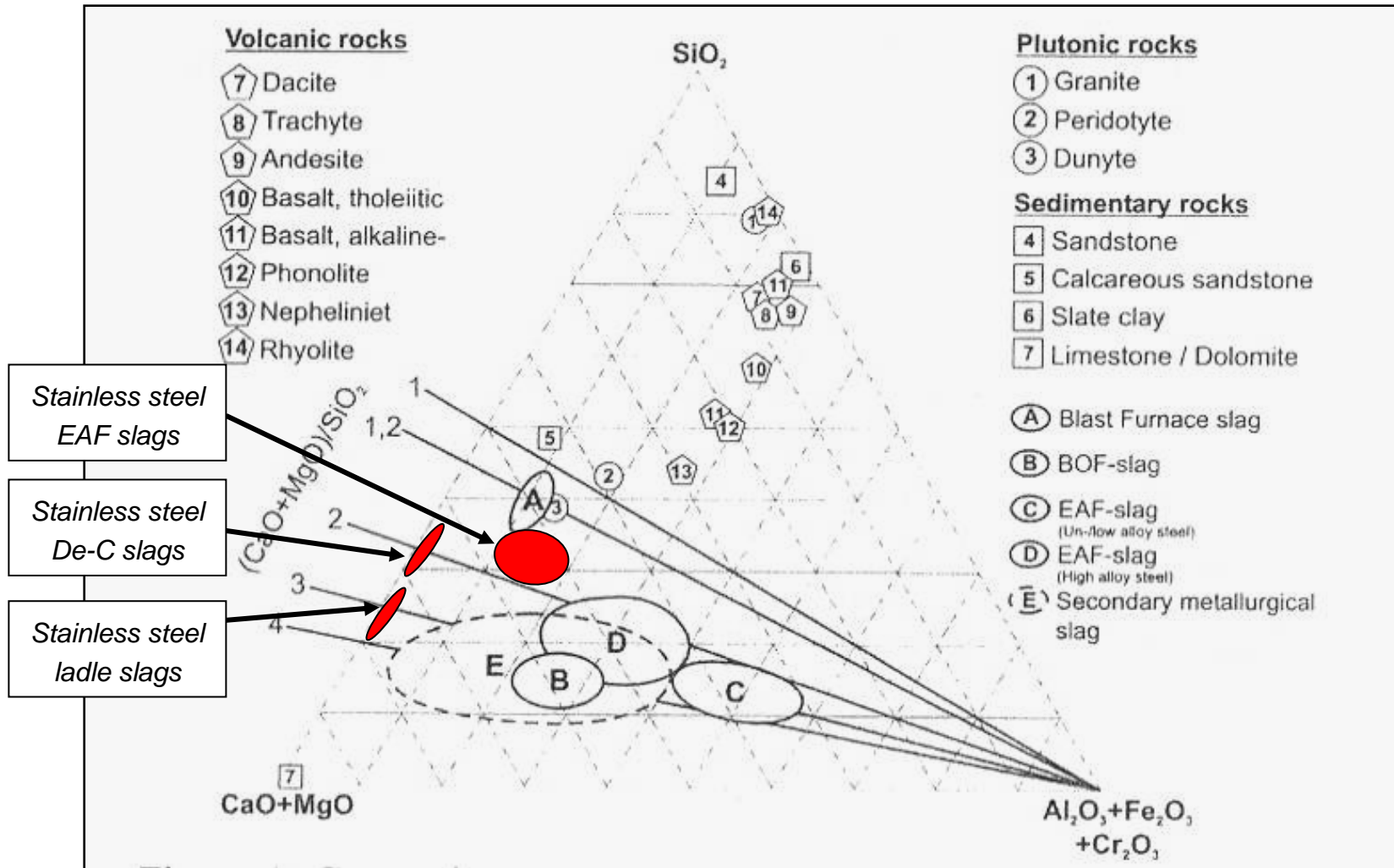
De-C slag

180 kg/ton steel

Ladle slag

20 kg/ton steel

Overview slag compositions



Motz and Kuhn., Scanmet II, 2004



Process Modelling: Chromium recovery and foaming in the EAF

S. Arnout, F. Verhaeghe, B. Blanpain, P. Wollants, R. Hendrickx, G. Heylen,, Steel Research International, 77 (5) (2006), 317 - 323

S. Arnout, D. Durinck, M. Guo. B. Blanpain, P. Wollants, J. American Ceramic Society, 91 (2008) 1237-1243

M.X. Guo, D. Durinck, P.T. Jones, G. Heylen, R. Hendrickx, R. Baeten, B. Blanpain, P. Wollants, Steel Research International, 78 (2) (2007), 117 - 124

D. Durinck, P.T. Jones, M.X. Guo, F. Verhaeghe, G. Heylen, R. Hendrickx, R. Baeten, B. Blanpain, P. Wollants, Steel Research International, 78 (2) (2007), 125 – 135



Slag in the EAF

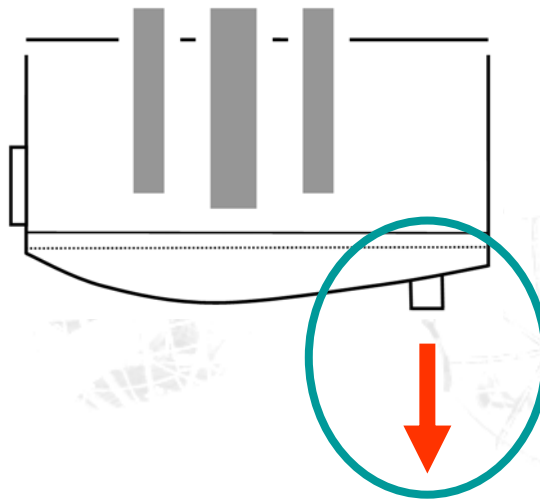


The EAF process

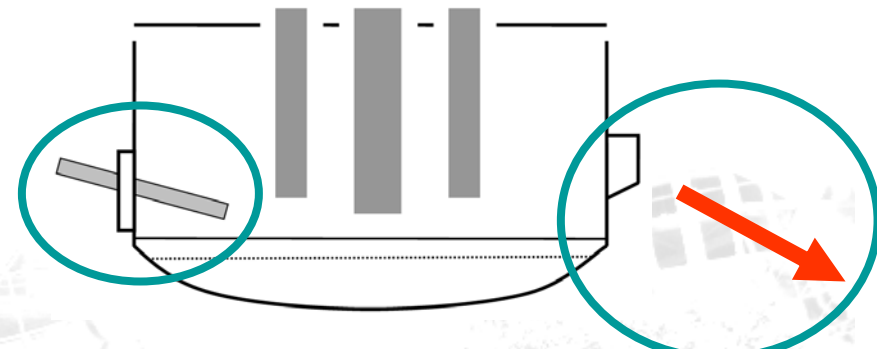
- Slag issues during EAF refining
 - Early liquid slag formation → prevent over-oxidation of Cr
 - Slag foaming → increase furnace productivity, refractory lifetime, energy and material efficiency
 - Chromium recovery → economical & environmental reasons
 - Immobilisation of CrO_x → enhance slag valorisation potential
- All affected by high-T slag microstructure

Furnace types

- Two distinct 120t EAFs
 - EAF1 = Eccentric Bottom Tapping Furnace
No C/O₂ lance → no foaming
 - EAF2 = Spout Tapping Furnace
C/O₂ lance → slag foaming



EAF1 (EBTF)

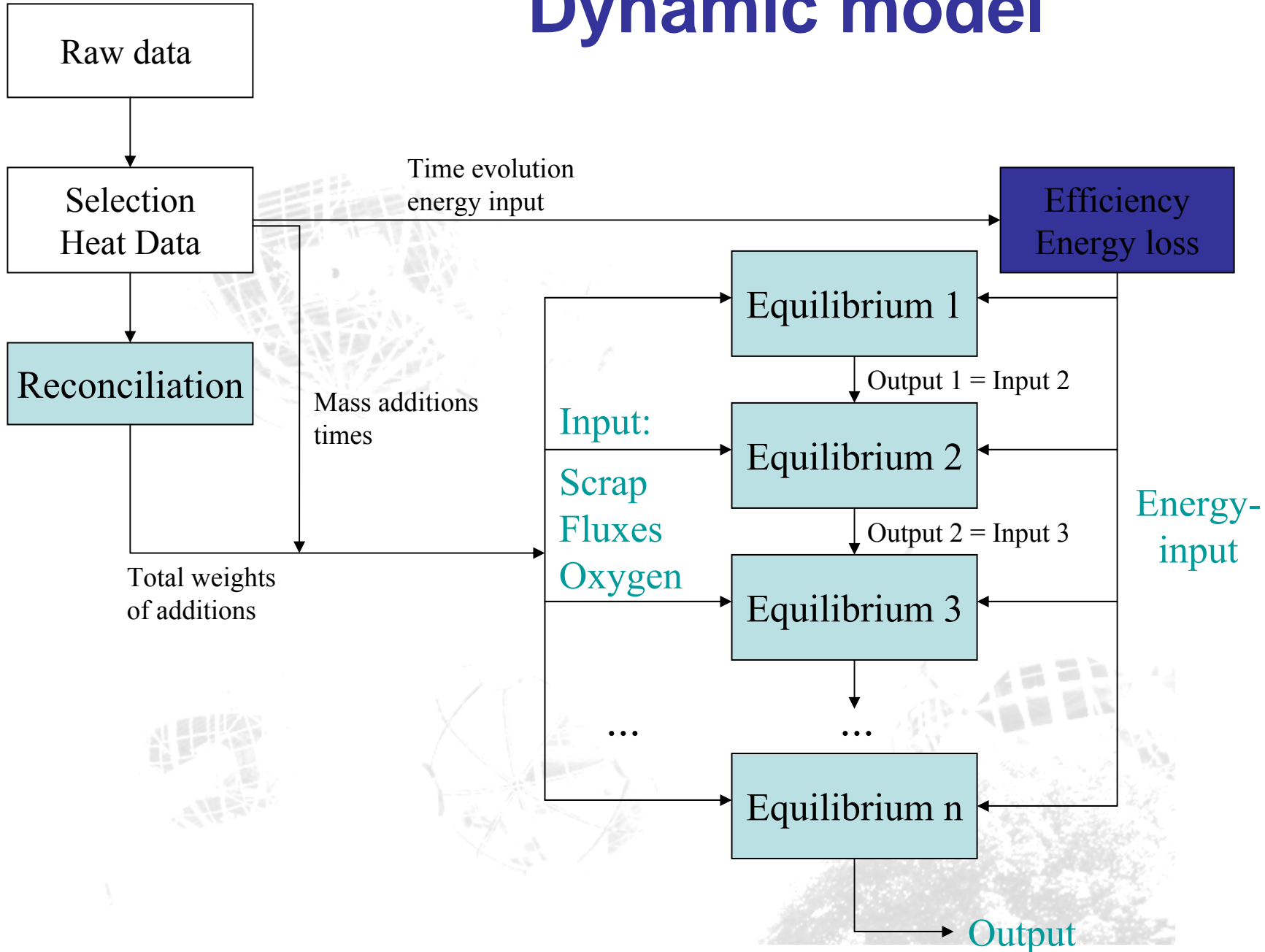


EAF2 (STF)

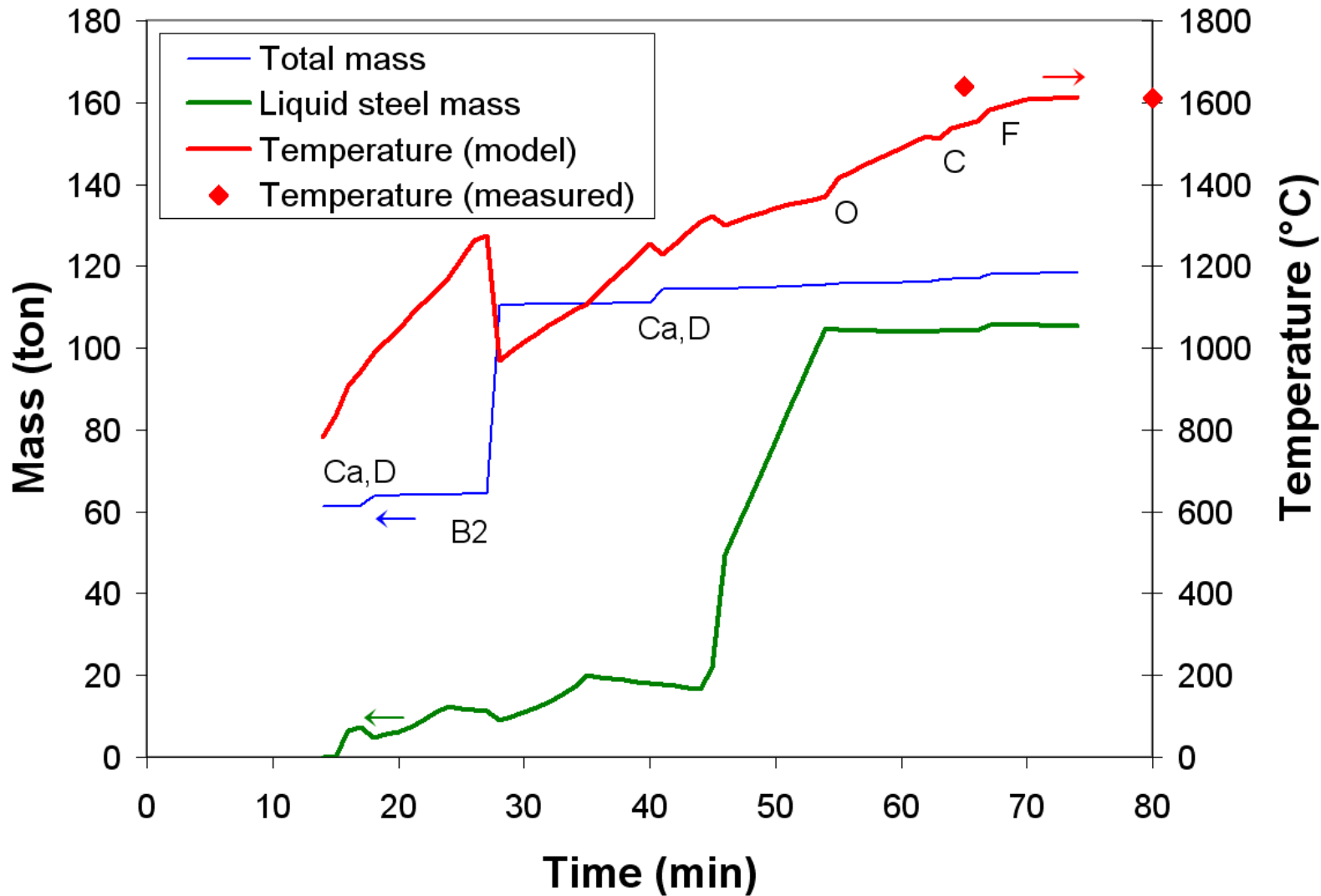
EAF operations

Min.	Operation	Min.	Operation	Abbr.
1-6	Charging 1st bucket			B1
7-26	Arc on	12	Start of calculations	S
		17-20	Calcia additions	Ca
		18	Dolomite and chamotte add.	D
28	Charging 2nd bucket			B2
29-70	Arc on	41	Dolomite and calcia addition	Ca,D
		49-63	Calcia additions	Ca
		55	O ₂ injection	O
		63	C/O ₂ injection	C
		67	Fe-Si and fluorspar addition	F
74	Tapping			T

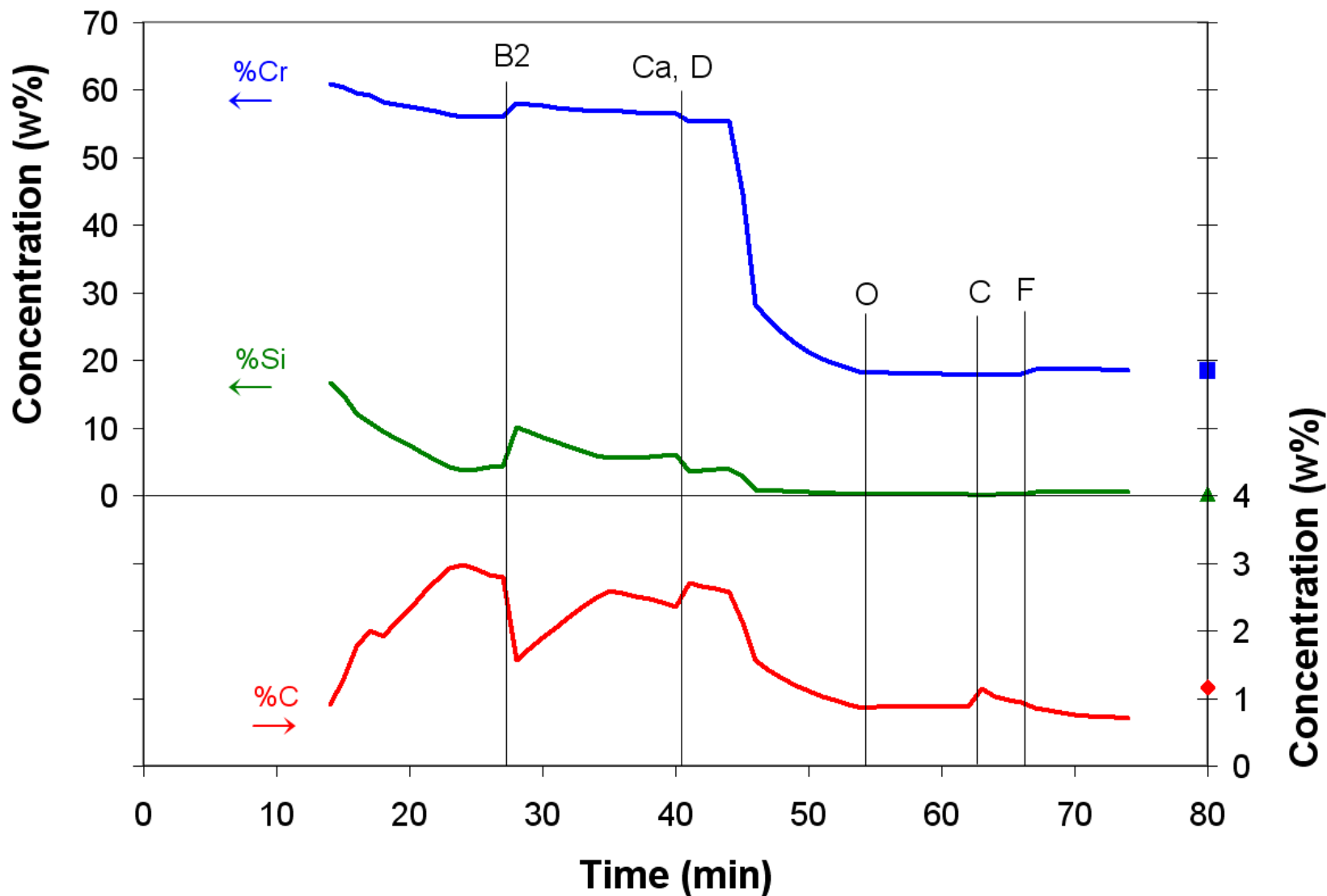
Dynamic model



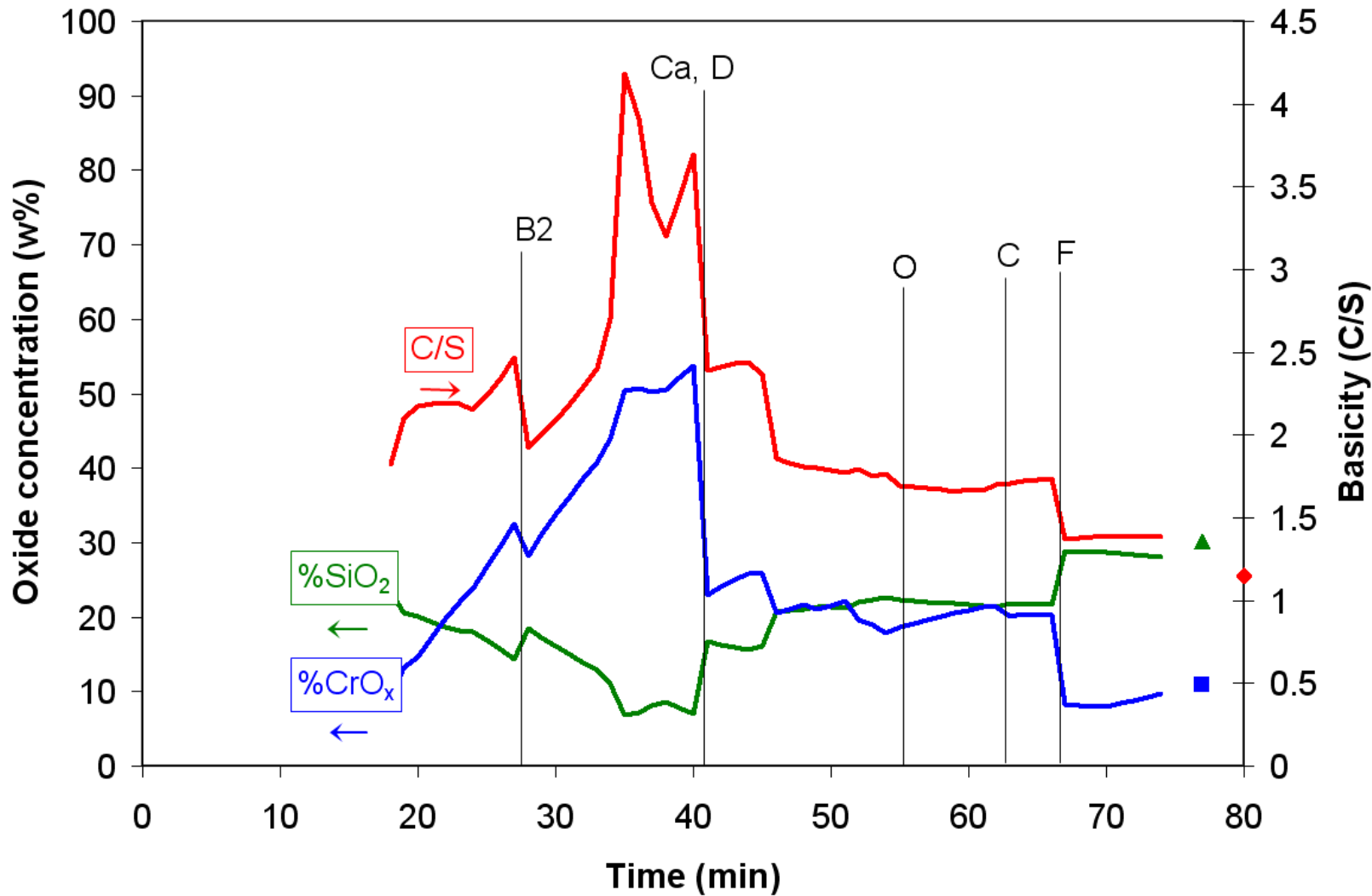
Temperature evolution



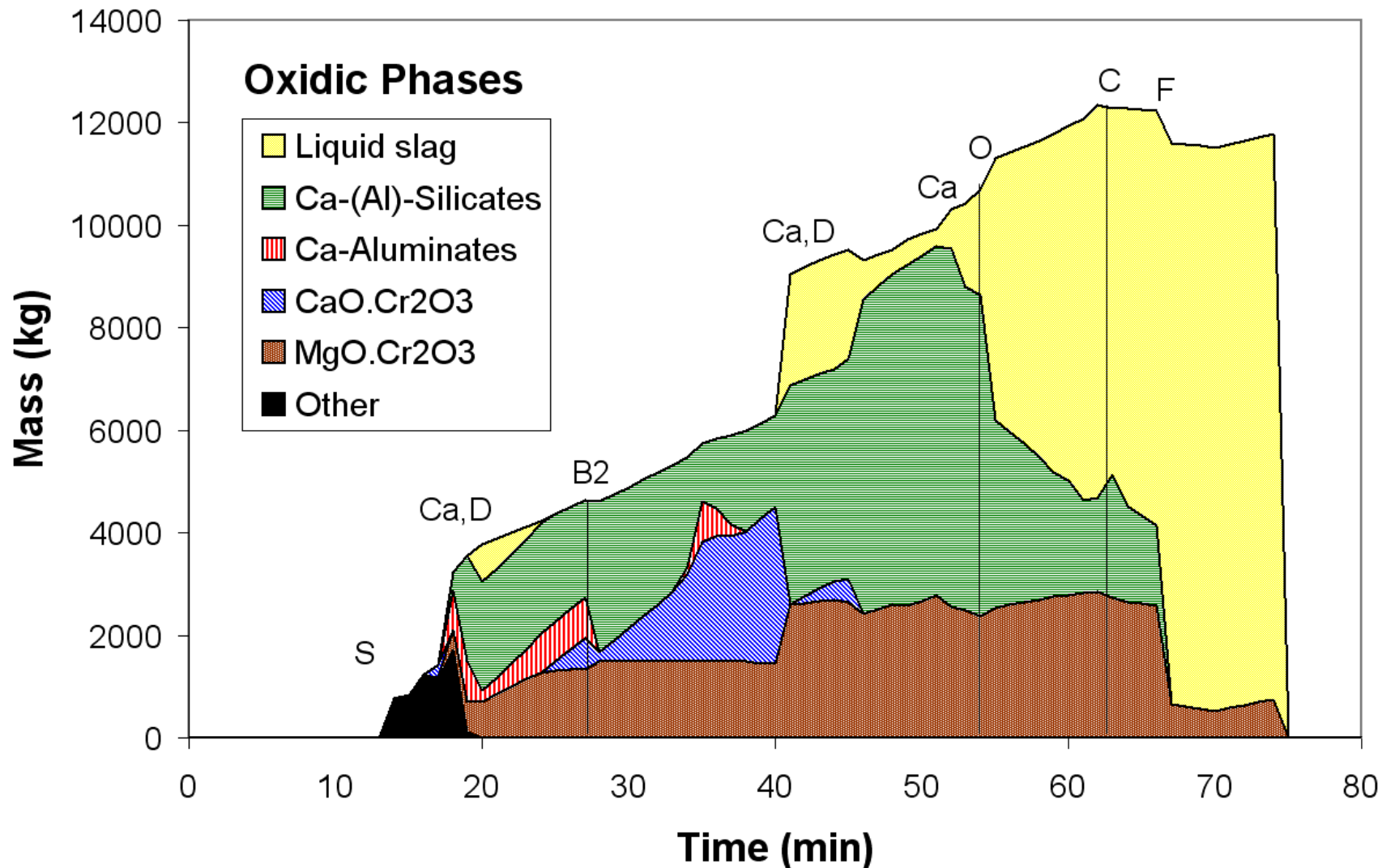
Steel composition



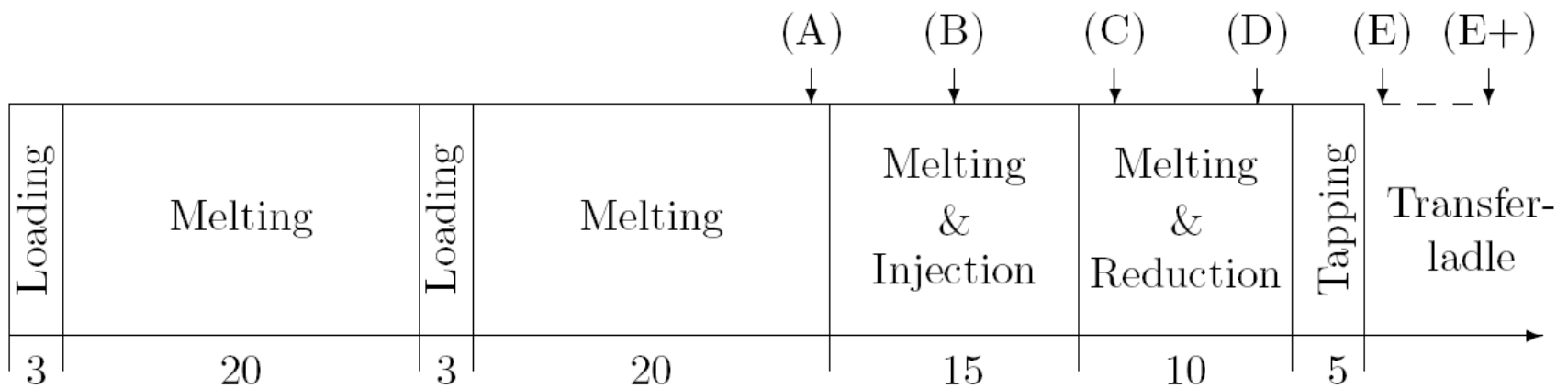
Slag composition



Phases in the slag



Slag Sampling



Schematic diagram of EAF process (STF) and sampling moments

Results – Evolution slag composition

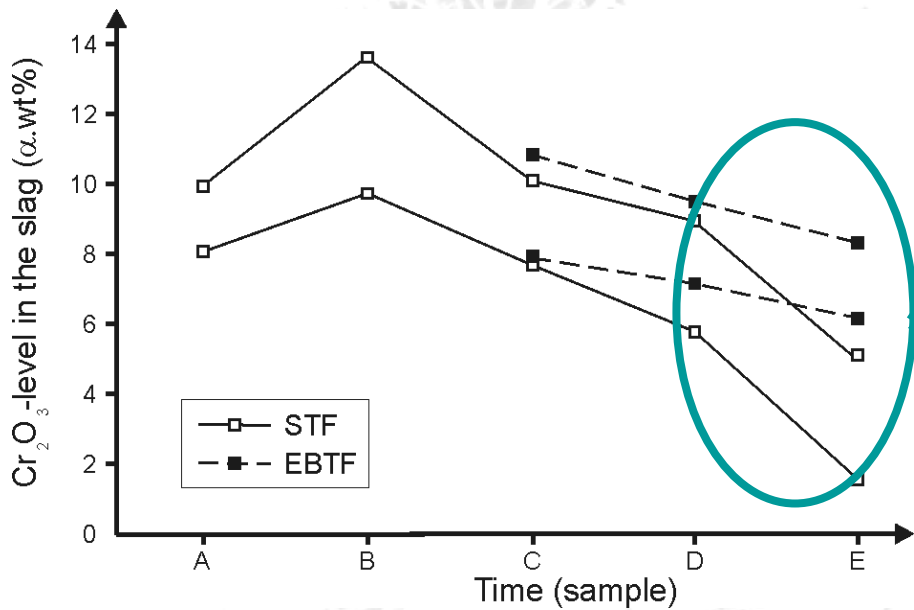
- Evolution in STF-slag composition:
 - (C+M)/S (basicity) decreases during process (FeSi additions for Cr-recovery)
 - FeO drops significantly
 - CrO_x mainly drops during tapping
- Evolution in EBTF-slag composition:
 - Higher final CrO_x levels due to tapping procedure

Observed range of global slag composition during STF-process

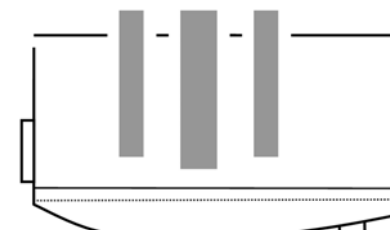
Results – Final CrO_x values (tapping)

Difference in Cr recovery due to tapping procedure

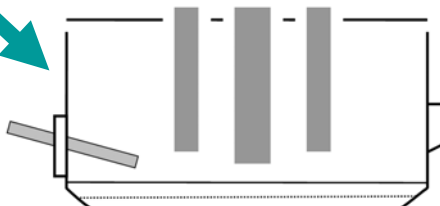
- EBTF: poor mixing
- STF: excellent mixing



Evolution 'Cr₂O₃' level (global slag composition) during STF-process

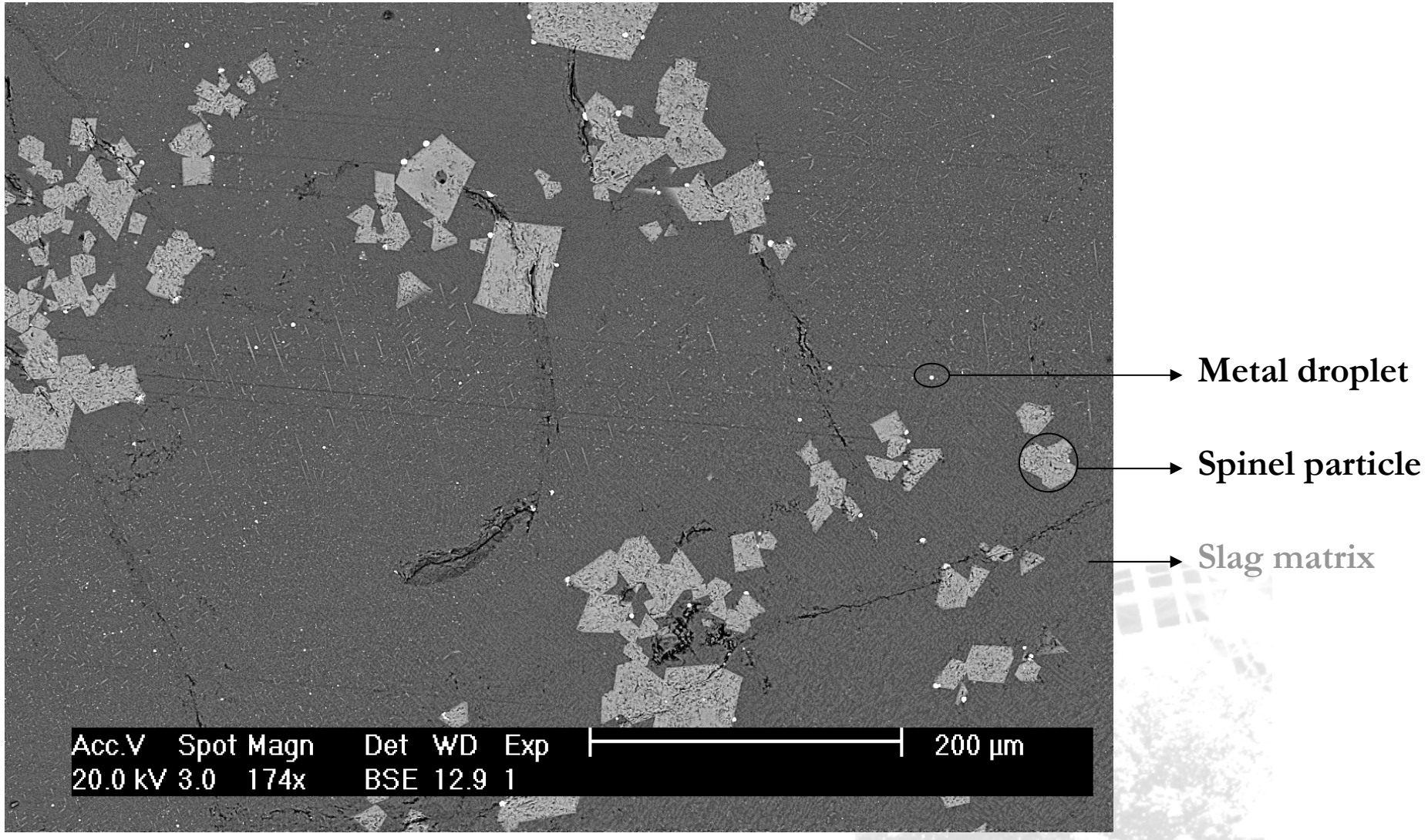


EBTF tapping:
first steel, then
slag, poor mixing
in transfer ladle

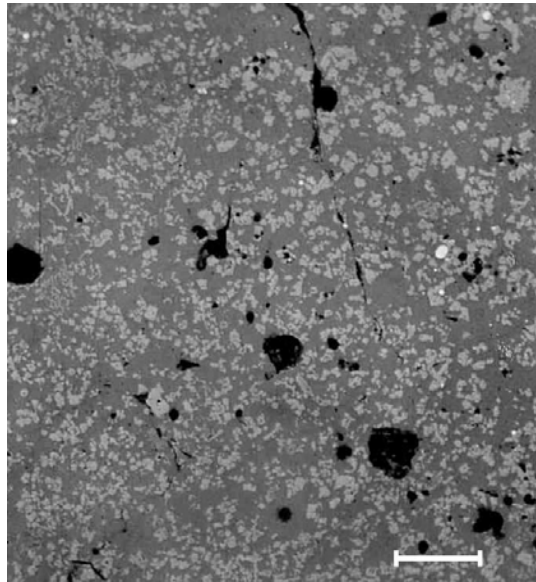


STF tapping: first slag,
then steel, good mixing
in transfer ladle

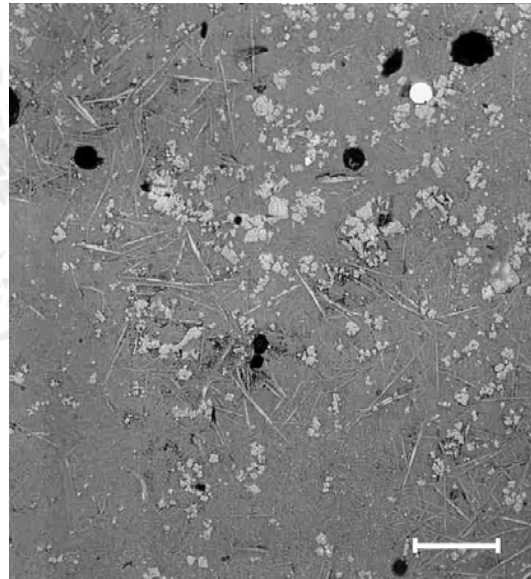
Slag microstructure



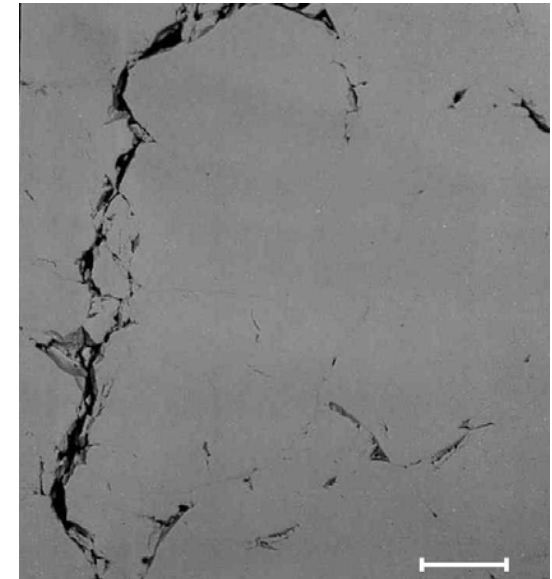
Results – Evolution slag microstructure



STF – Before blowing
(bar = 250 μm)

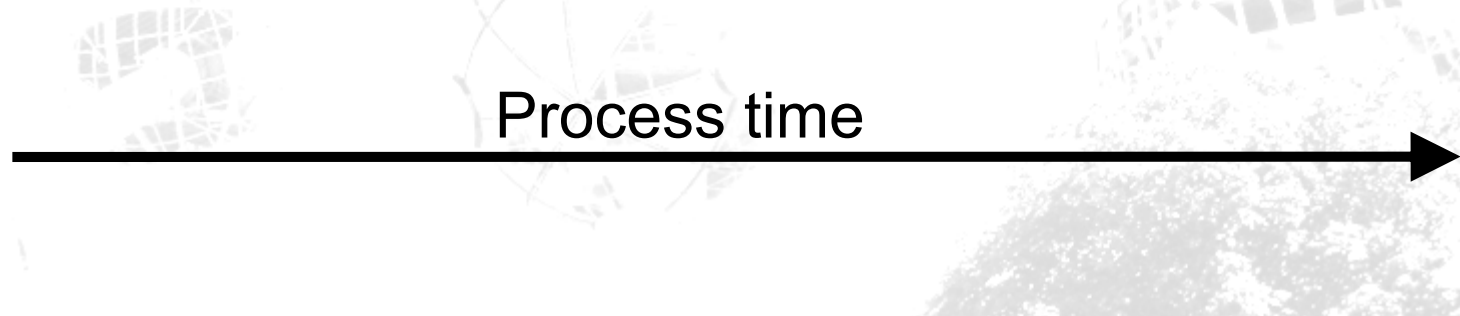


STF – After blowing
(bar = 250 μm)



STF – After tapping
(bar = 250 μm)

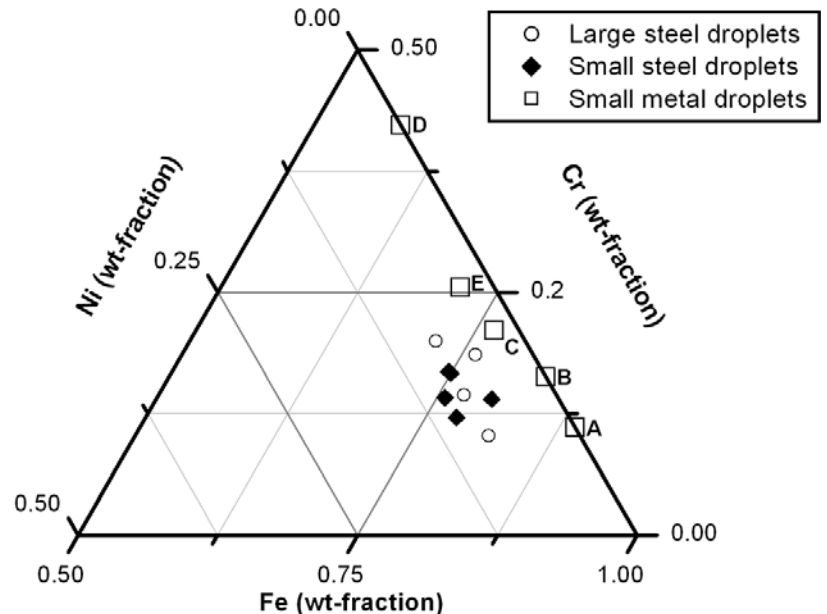
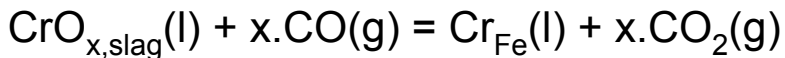
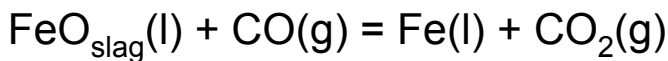
Process time



Slag microstructure – metal droplets

- Type 1: large ($>50 \mu\text{m}$): stainless steel particles (originating from steel bath)

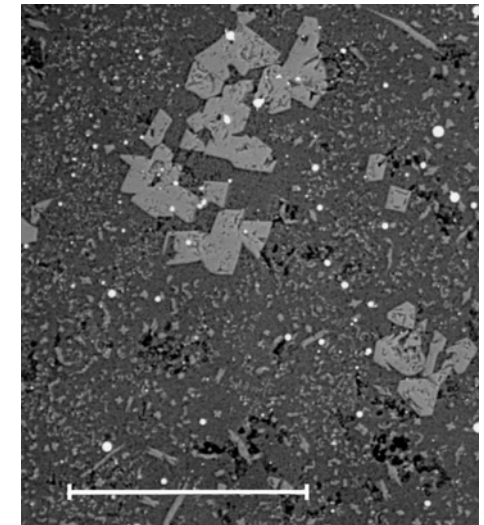
- Type 2: small ($< 5 \mu\text{m}$)
 - Type 2a (25%): stainless steel composition
 - Type 2b (75%): Fe/Cr (no Ni) from two reactions:



Composition metallic droplets in the slag

Slag microstructure – spinel particles

- Size: ~20 µm, shape: angular
- Present at high temperature
- Composition: $(\text{Mg}, \text{Fe}, \text{Mn})\text{O} \cdot (\text{Cr}, \text{Al})_2\text{O}_3$
- Evolution in composition (see table)
- Amount of particles decreases with process time (~ FeSi addition & Cr-recovery)
- STF-samples after tapping: almost no particles left



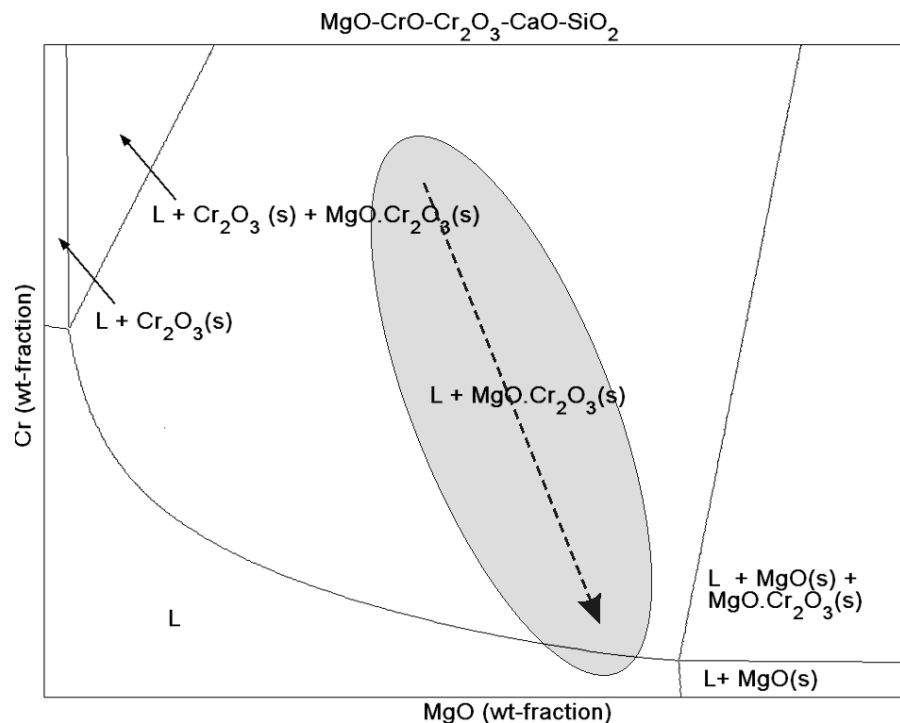
Spinel particles in slag
(bar = 100 µm)

Compositional evolution spinel particles during STF-process

Sample		Cr^{3+}	Al^{3+}	Mg^{2+}	Fe^{2+}	Mn^{2+}	Ca^{2+}	$\text{M}^{3+}/\text{M}^{2+}$
448032	A	25.0	2.6	6.4	5.9	1.8	0.9	1.8
448032	B	25.0	2.7	7.4	2.2	2.9	1.4	2.0
448032	C	24.9	3.6	8.3	0.8	3.4	0.9	2.1
448032	D	24.9	3.5	9.2	1.1	2.5	0.9	2.1
448032	E	19.5	6.3	12.3	0.3	1.6	0.7	1.8

Slag microstructure – spinel particles

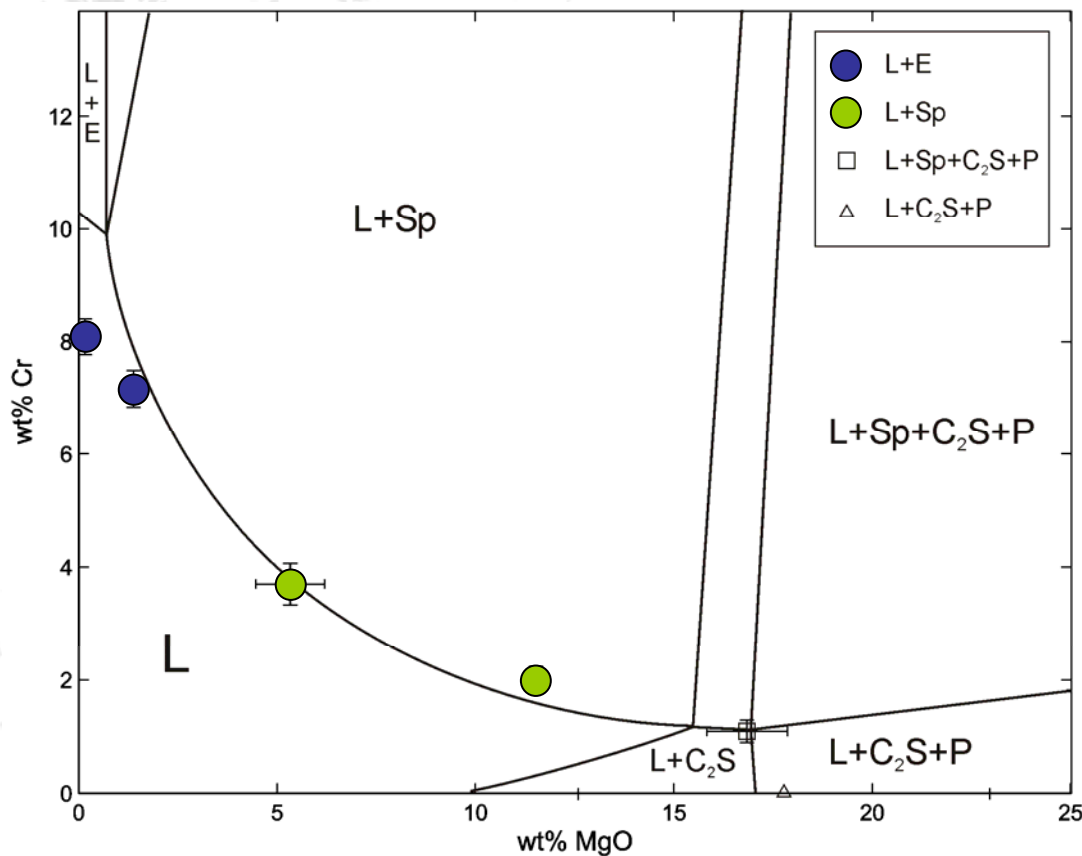
- Formation and dissolution of spinel particles controlled by:
 $\text{Cr}_2\text{O}_3/\text{Al}_2\text{O}_3 \text{ (l)} + \text{MgO} \text{ (l)} \rightleftharpoons \text{MgO} \cdot (\text{Cr}, \text{Al})_2\text{O}_3 \text{ (s)}$
- Equilibrium influenced by T, pO₂ (influences CrO/Cr₂O₃ level), C+M/S, CrO_x and MgO level
- FactSage 5.2 + Chemapp V5.1.6 → qualitative phase diagram
- Process evolution shown by arrow: from L/spinel → L region without spinel



Qualitative phase diagram: C/S, p, p_{O₂} and T are kept constant

Results: liquidus

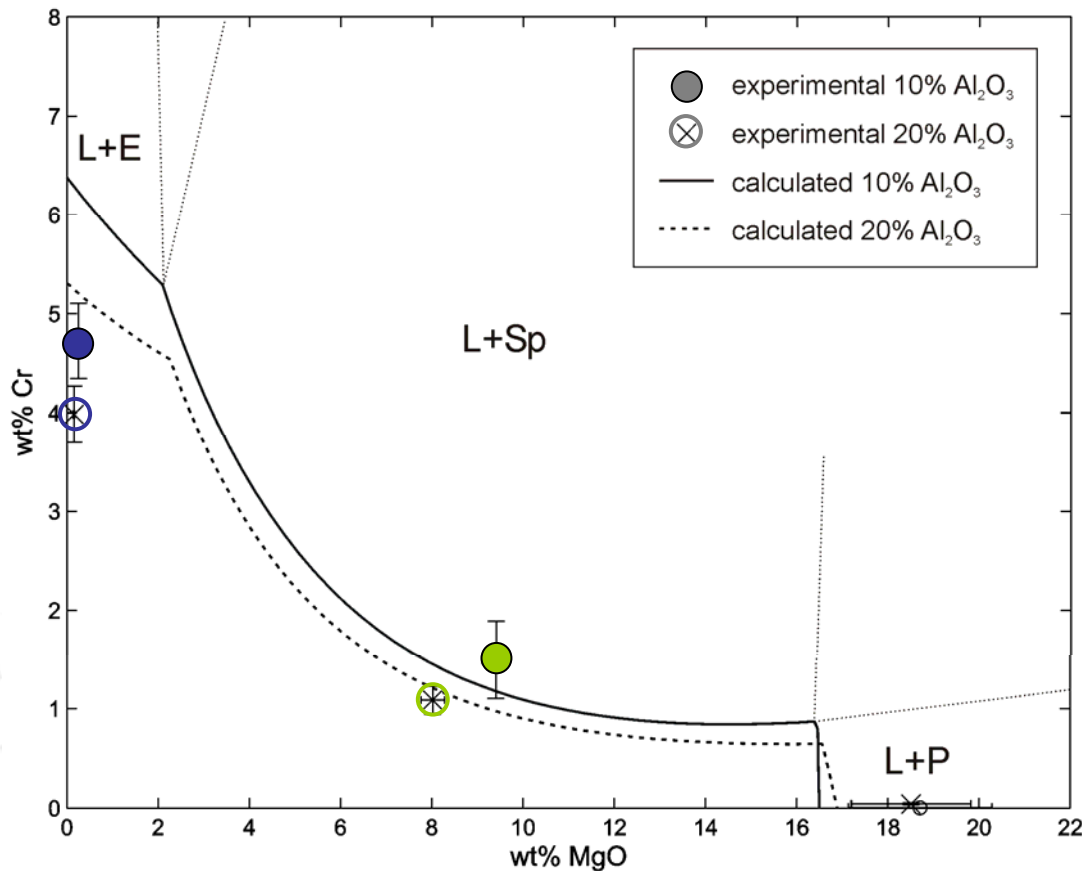
- Tests in different known p_{O_2} , no Al_2O_3



$T = 1600^\circ C$
 $p_{O_2} = 10^{-10.16}$ atm
 $B = 1.2$

Results: liquidus

- Tests in known p_{O_2} , changing Al_2O_3



$T = 1600^\circ C$
 $p_{O_2} = 10^{-9.36} \text{ atm}$
 $B = 1.2$

Other examples of process modelling

- VOD stainless steel refining
 - S. Smets et al., unpublished.
- Zinc fuming (including freeze lining formation)
 - Cooperation with E. Jak and P. Hayes
 - K. Verscheure et al., Met. Trans. B, 38B (2007), 13 – 33
- Lead Blast Furnace
 - Cooperation with E. Jak and P. Hayes
 - F. Verhaeghe et al., Proc. CSIRO, 4th Australian Melt Chemistry Symposium , 10-11 December 2002
- Exergy analysis of pyrometallurgical processes
 - B. Klaasen et al, master thesis K.U.Leuven, 2008 (in dutch)



Slag Valorisation: the importance of microstructure

Roadways to a stable slag product

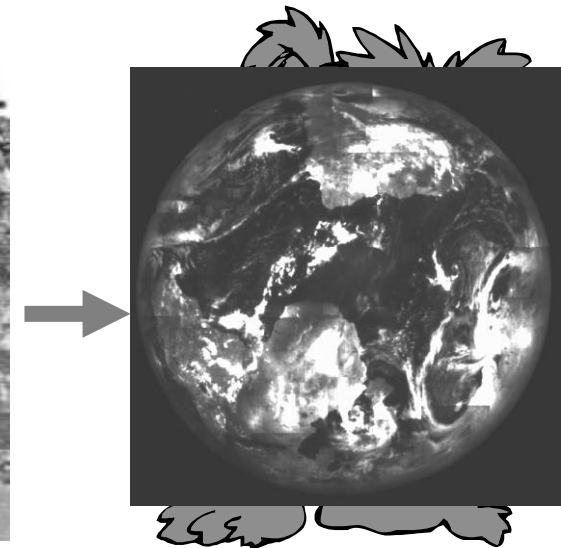
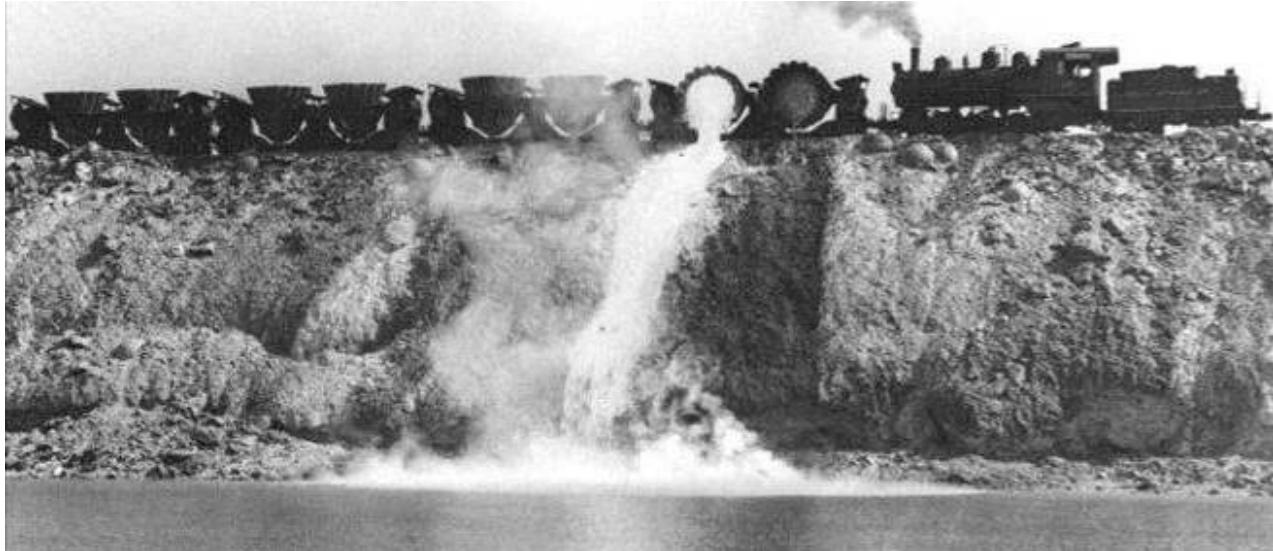
D. Durinck, S. Arnout, G. Mertens, E. Boydens, P.T. Jones, J. Elsen, B. Blanpain, P. Wollants,
JOURNAL OF THE AMERICAN CERAMIC SOCIETY 91(2008) 548-554

D. Durinck, P.T. Jones, B. Blanpain, P. Wollants, G. Mertens, J. Elsen, Journal of The American Ceramic Society, 90 (4) (2007), 1177 - 1185

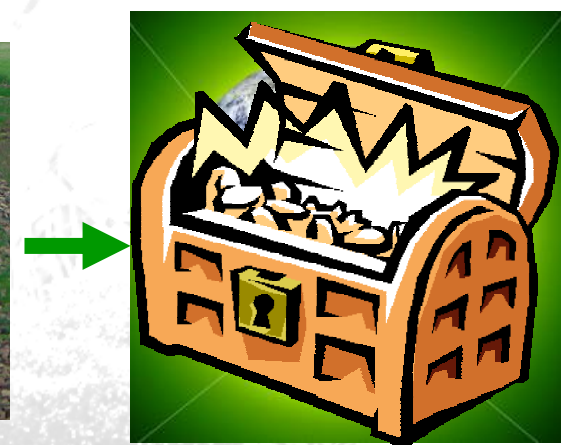




Dumping



Valorisation



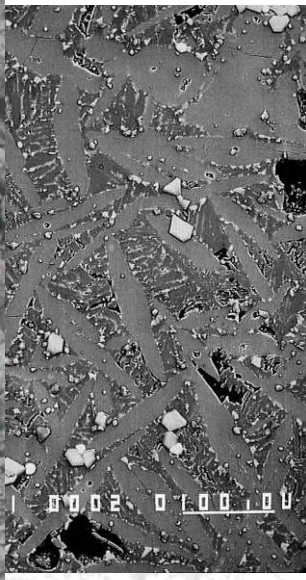
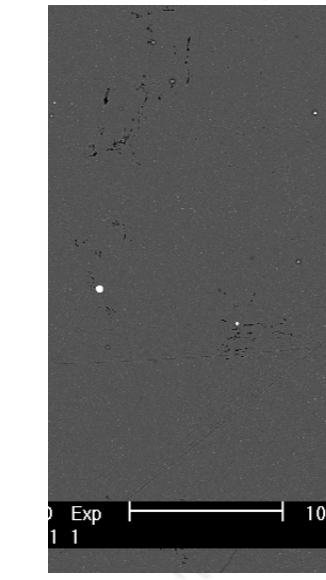
Slag valorisation chain



Slow slag solidification



0.45



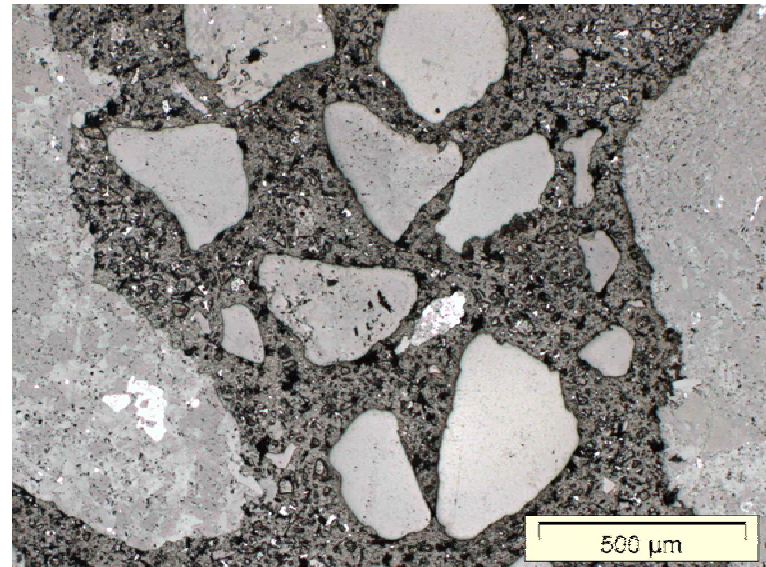
Slag valorisation chain

Main applications:

- Flemish environmental law:
“aggregates within other products”

→ Concretes

- Cementitious concrete
- Asphalt concrete



Slag valorisation chain

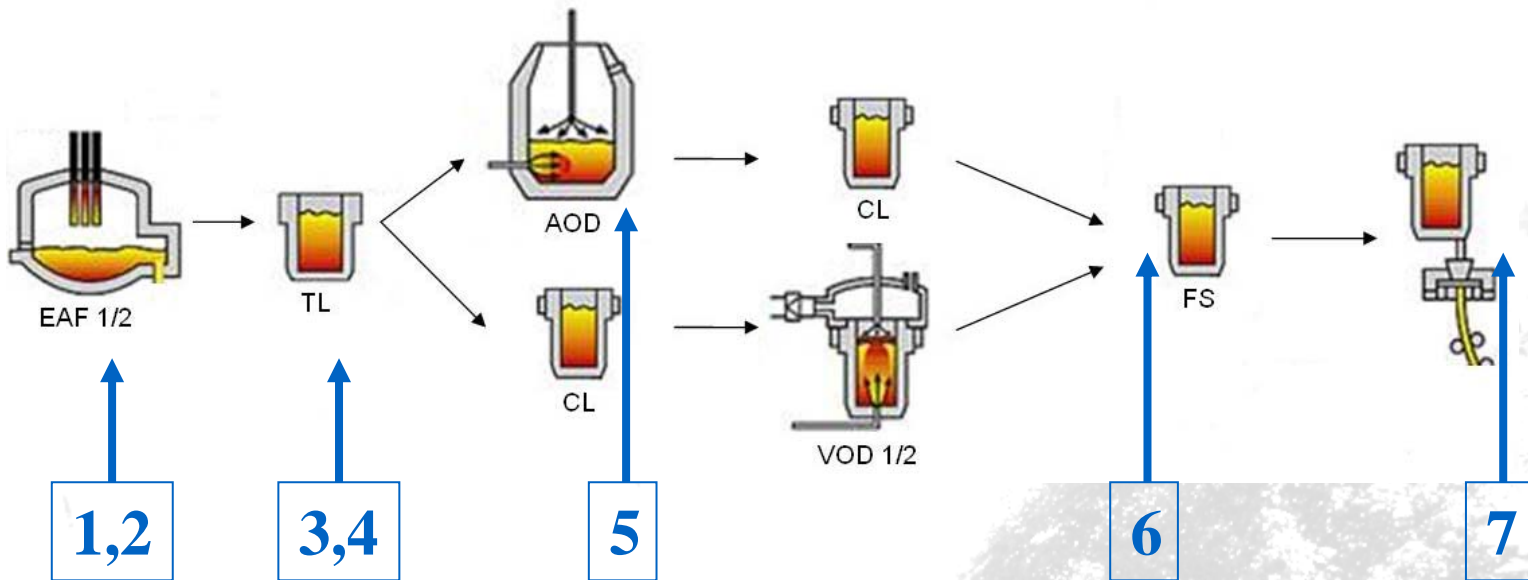
Required slag properties for aggregate for asphalt concrete:

- Particle size > 2 mm
- Resistance against polishing
- Abrasion resistance
- Strength
- Cr leaching
- Volume stability



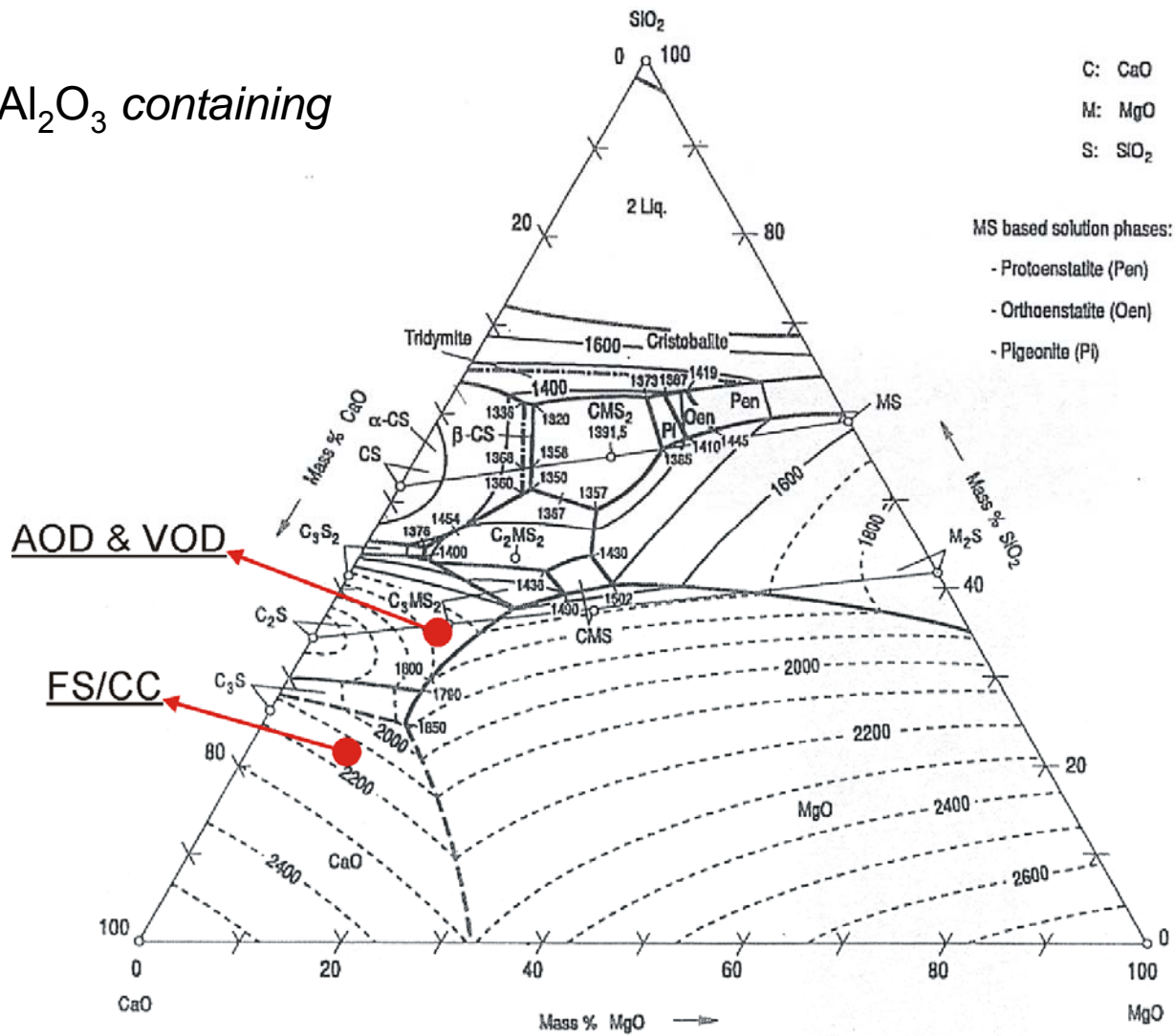
Slag composition

	'CaO'	SiO ₂	MgO	Al ₂ O ₃	Amount
	wt%				Ton slag/100 ton steel
DS1	40	26	7	9	6
DS2	40	30	11	9	7
AOD	51	34	11	1	8
VOD	51	34	11	1	5
FS/CC	64	21	9	1	2



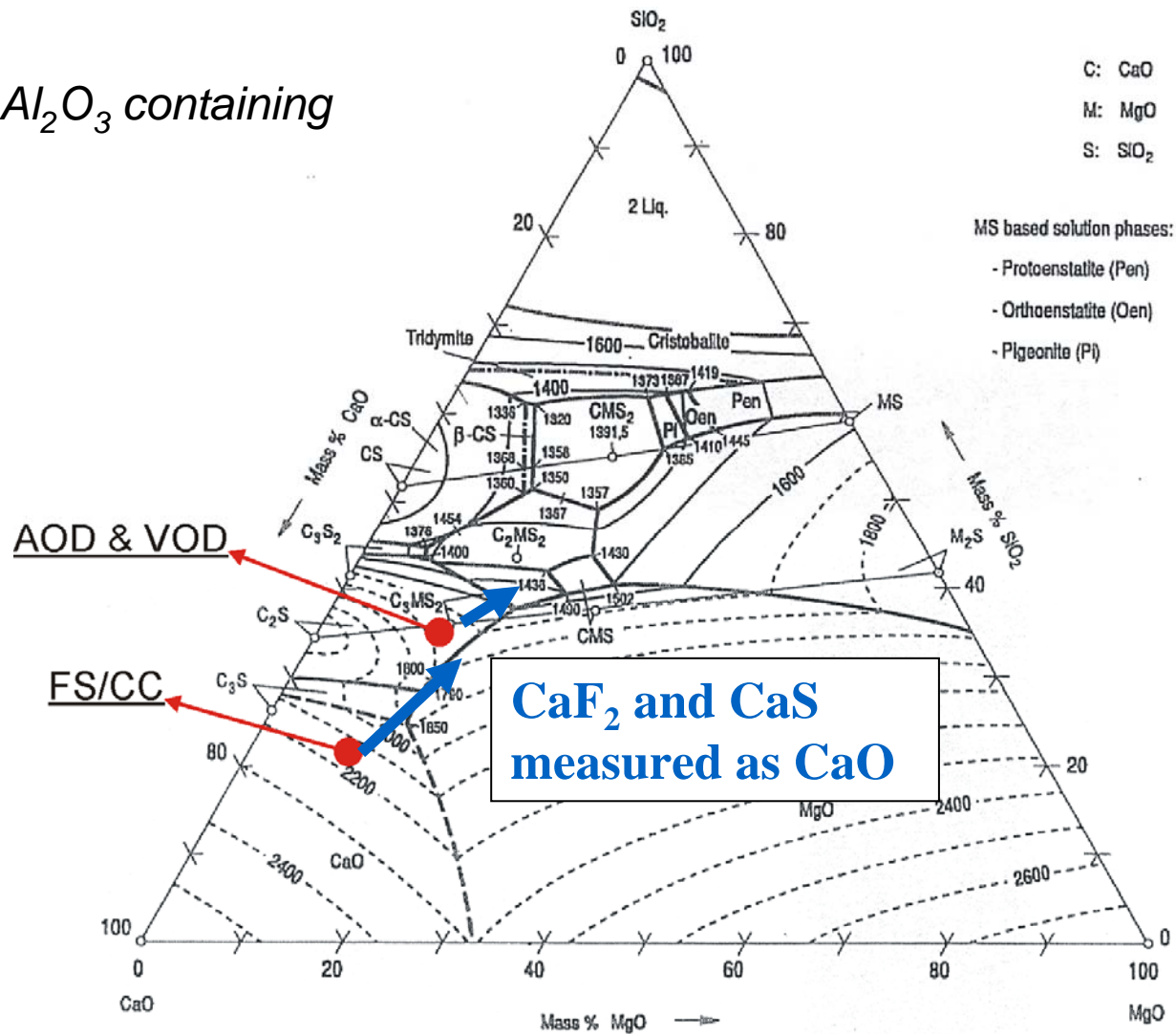
Slag composition

EAF = Al_2O_3 containing



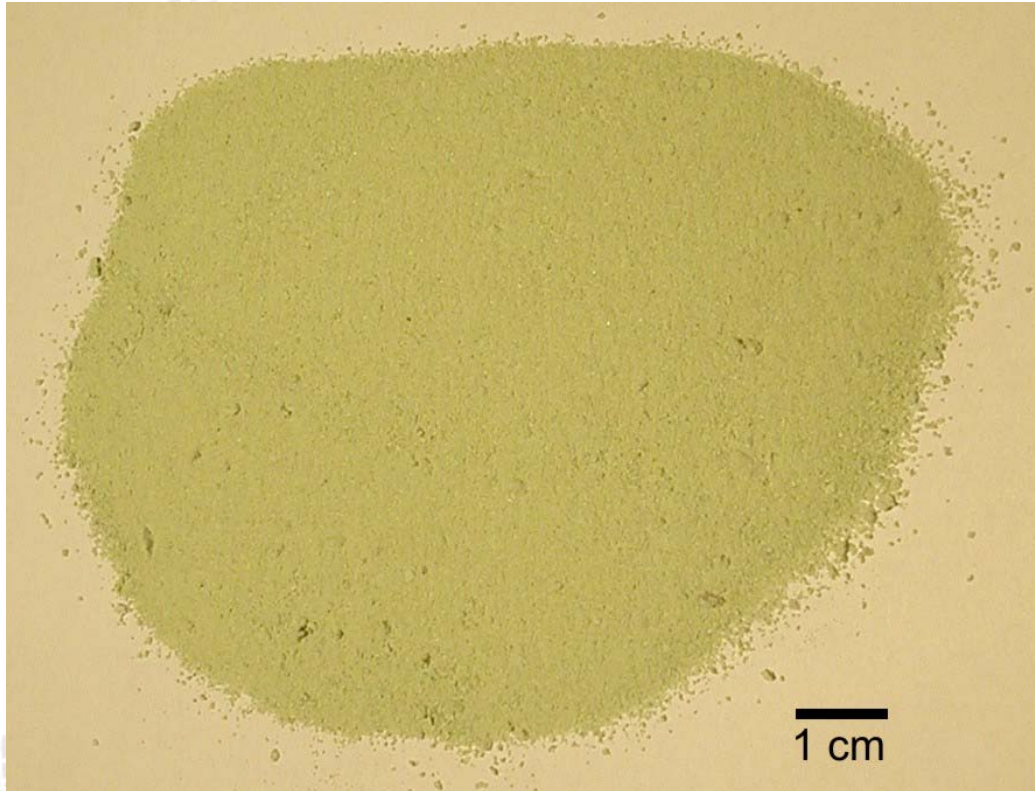
Slag composition

EAF = Al₂O₃ containing



Slag disintegration

- FS/CC slag after cooling: Too fine to valorise



Lab simulation

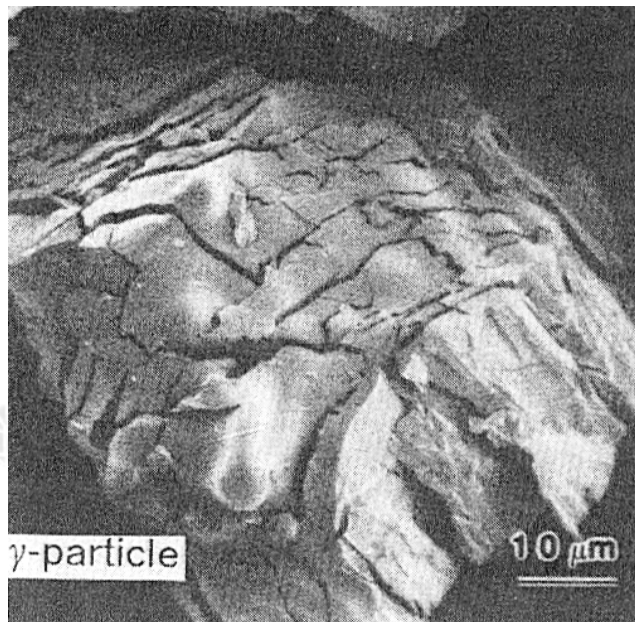
Slag disintegration

- Visual observation at the slag yard

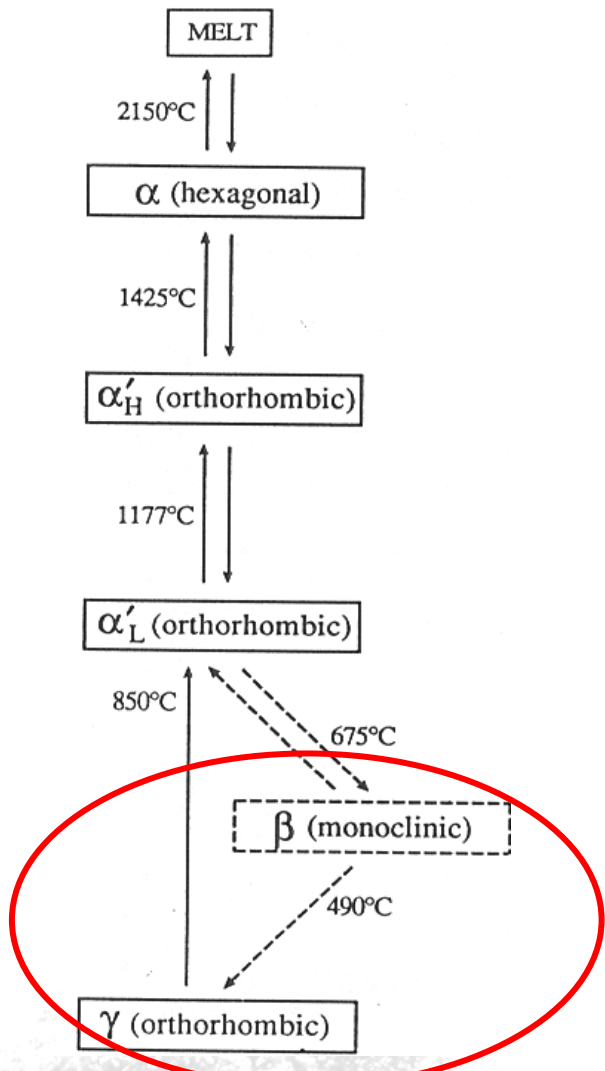


Cause of slag disintegration

- Presence of $2\text{CaO} \cdot \text{SiO}_2$ (C_2S)
 - several phase transformations during cooling
 - β to γ transformation causes a 12% volume expansion



Chan et al., J. Am. Cer. Soc., 1992



Kim et al., J. Am. Cer. Soc., 1992

What can be done?

□ Internal slag recycling

- Benefits: Ca resource, fluxing agent, possible heat source
- Problems: Logistics (dry slag required / molten slag addition)

□ Physical slag stabilisation

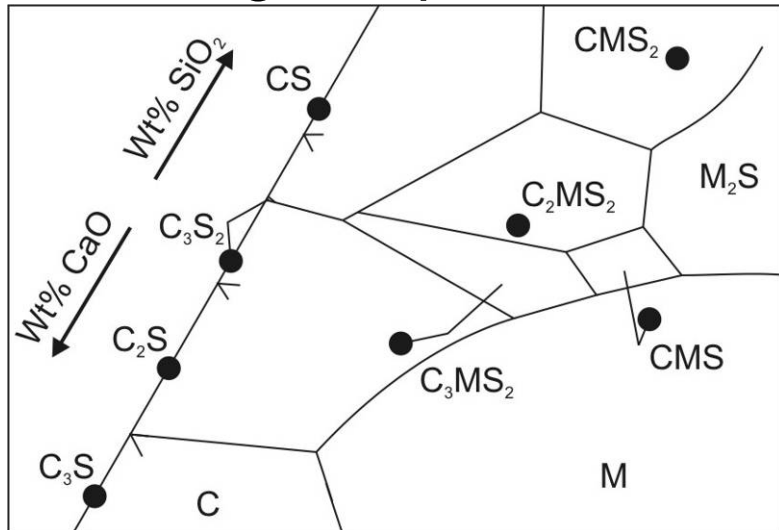
- Grain size
- Matrix constraint
- Cooling rate

□ Chemical slag stabilisation

- Stabilise $\beta\text{-C}_2\text{S}$ to room temperature by doping

Laboratory experiment

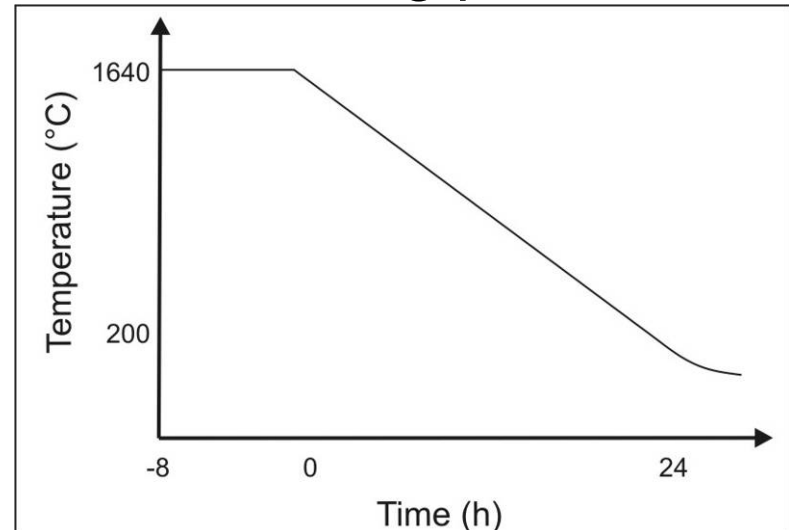
Slag composition



CaO-SiO₂-MgO

- Well known system
- p_{O_2} independent
- Stainless steelmaking slag
- Peritectic reaction

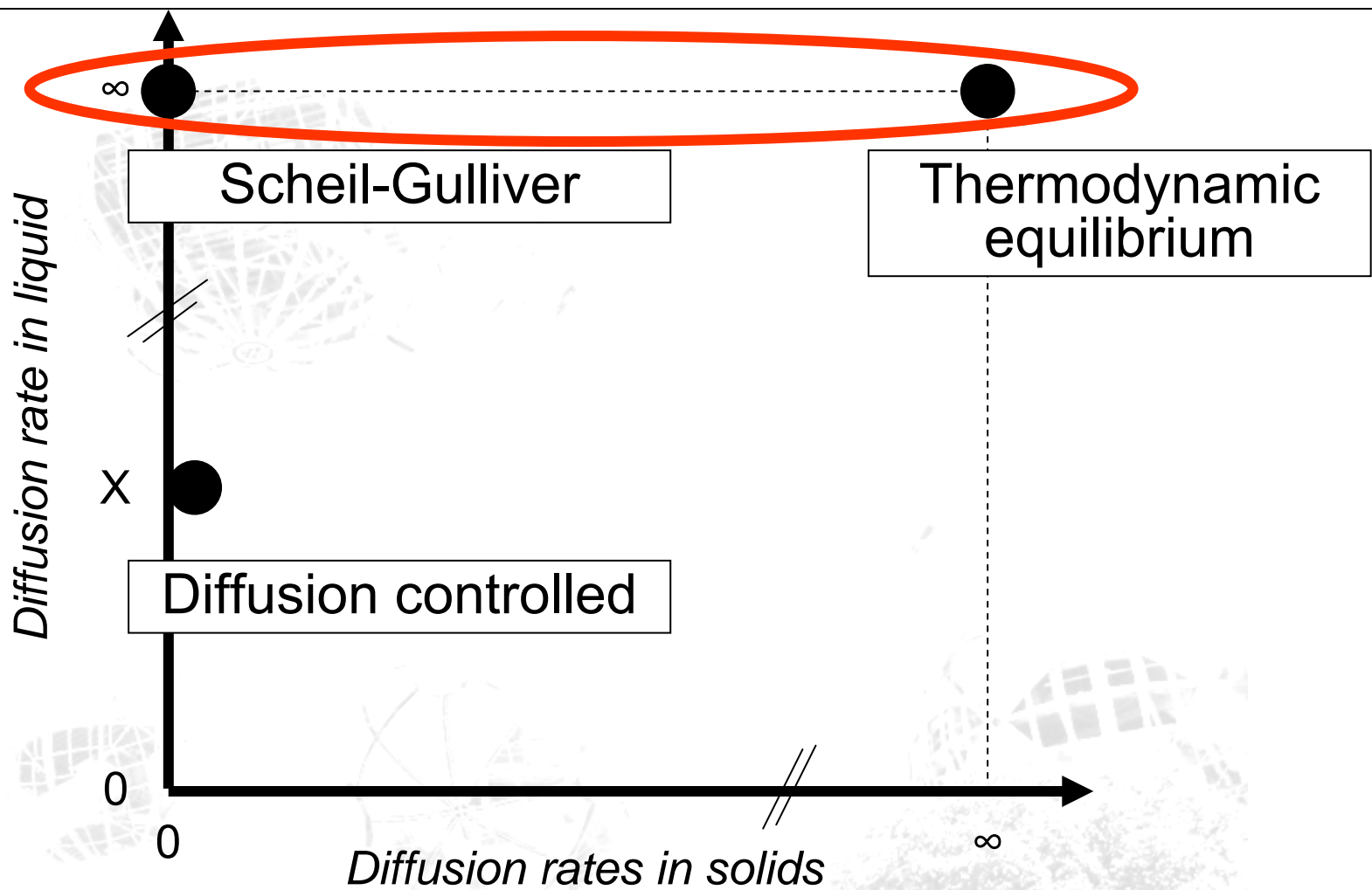
Cooling path



Cooling rate 1°C/min

- Simple cooling path
- Used in other references
- Comparable to industry
(not equal!)

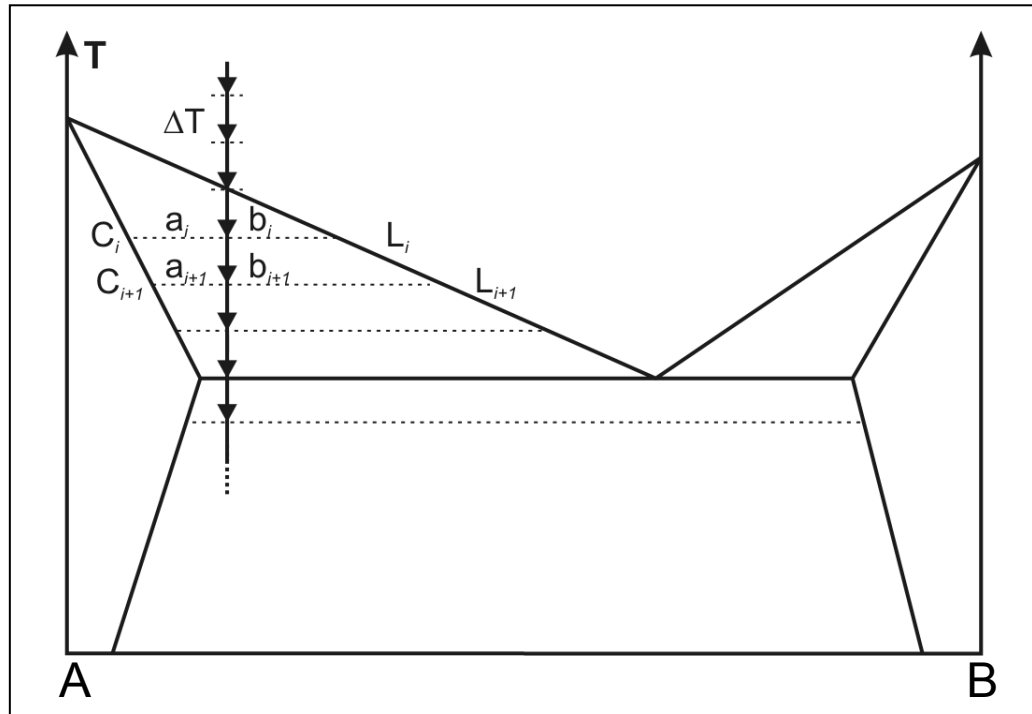
Common approaches to solidification modelling



Thermodynamic equilibrium model

Assumptions

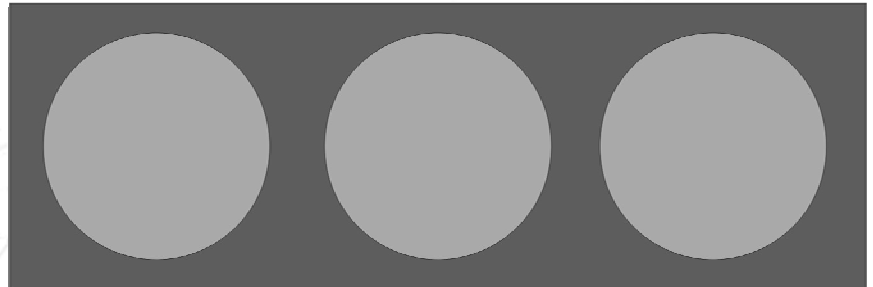
- Equilibrium @ L/S interface
- Infinitely rapid diffusion in L
- Infinitely rapid diffusion in S



Amount of A:

$$f_{s, \text{equil}} = \frac{b_i}{a_i + b_i}$$

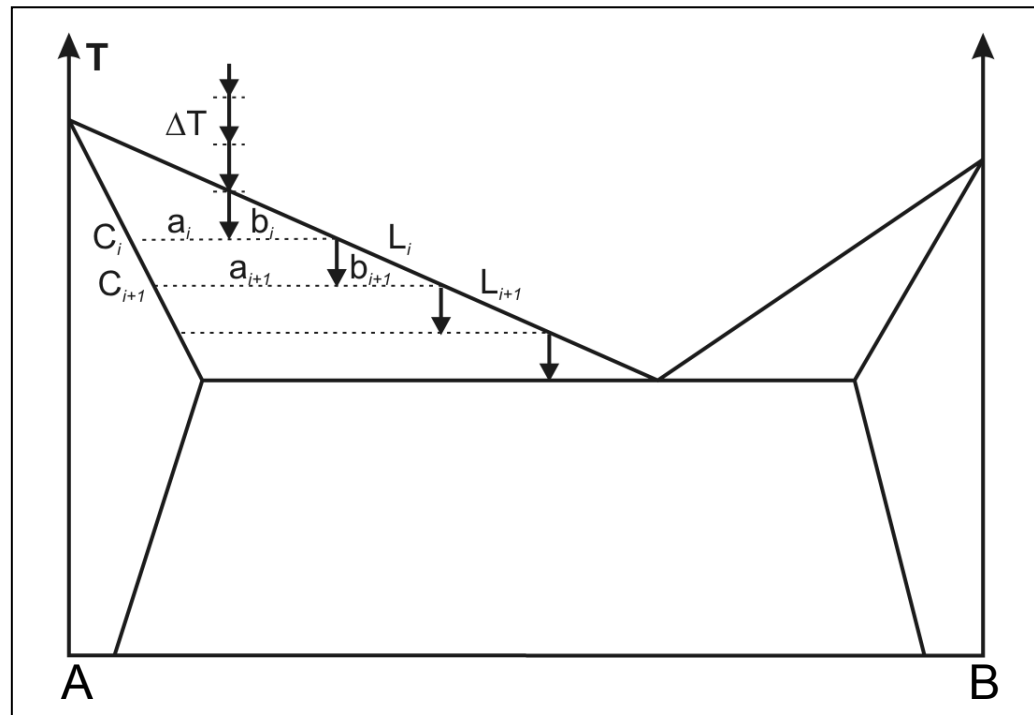
$$T_1 > T_2 > T_3 > T_4$$



Scheil-Gulliver model

Assumptions

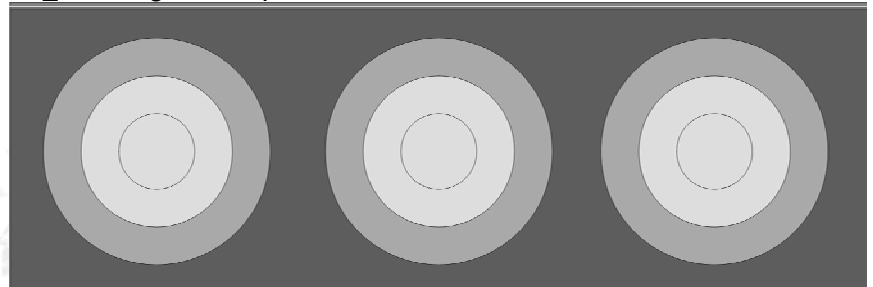
- Equilibrium @ L/S interface
- Infinitely rapid diffusion in L
- No diffusion in S



Amount of A:

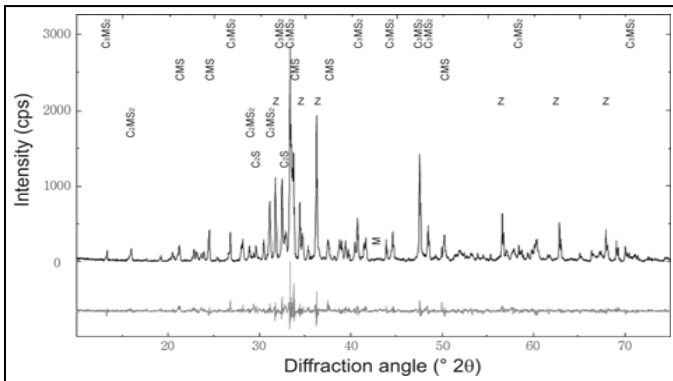
$$f_{s,SG} = \sum_{i=1 \rightarrow N} \frac{b_i}{a_i + b_i}$$

$$T_1 > T_2 > T_3 > T_4$$

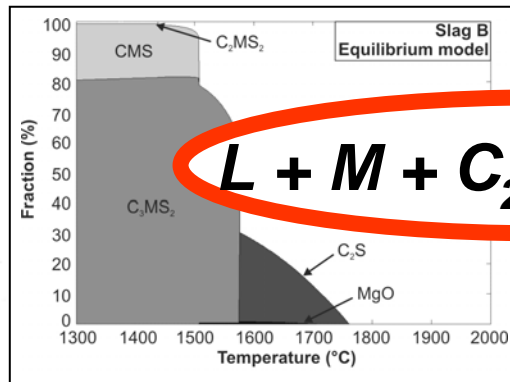


Mineralogy

Experiment

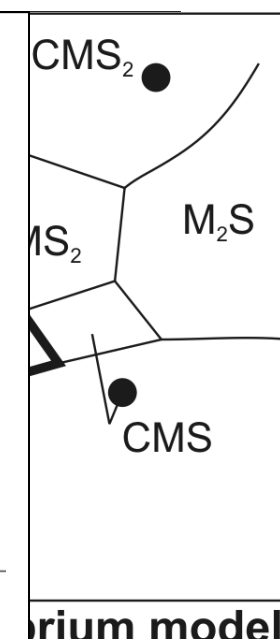
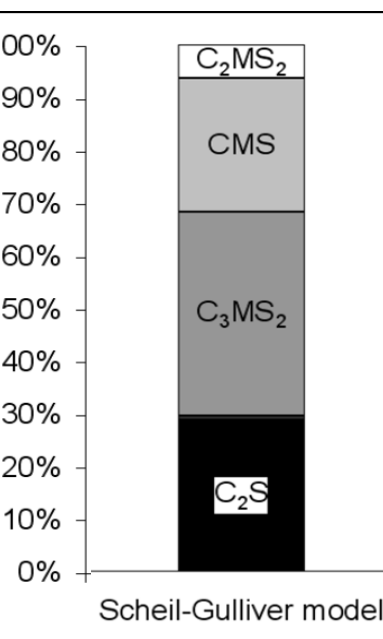
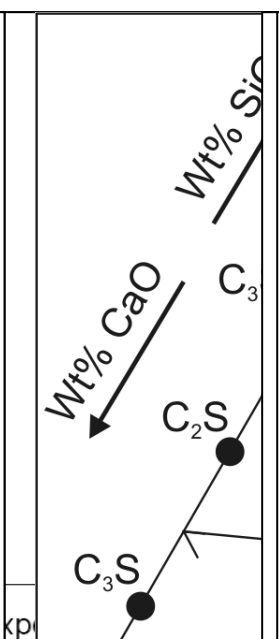
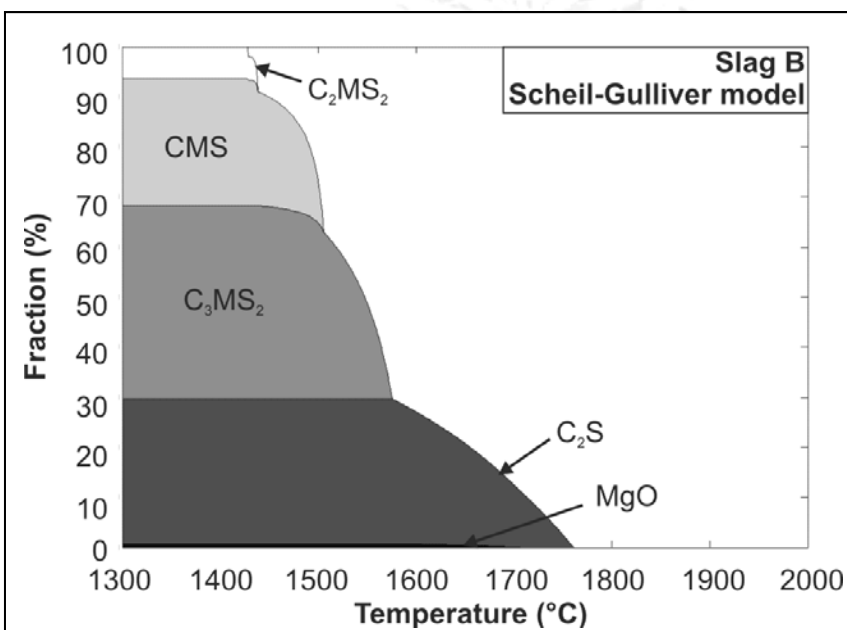
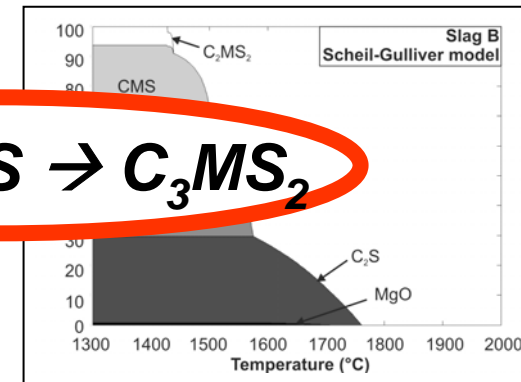


Equilibrium

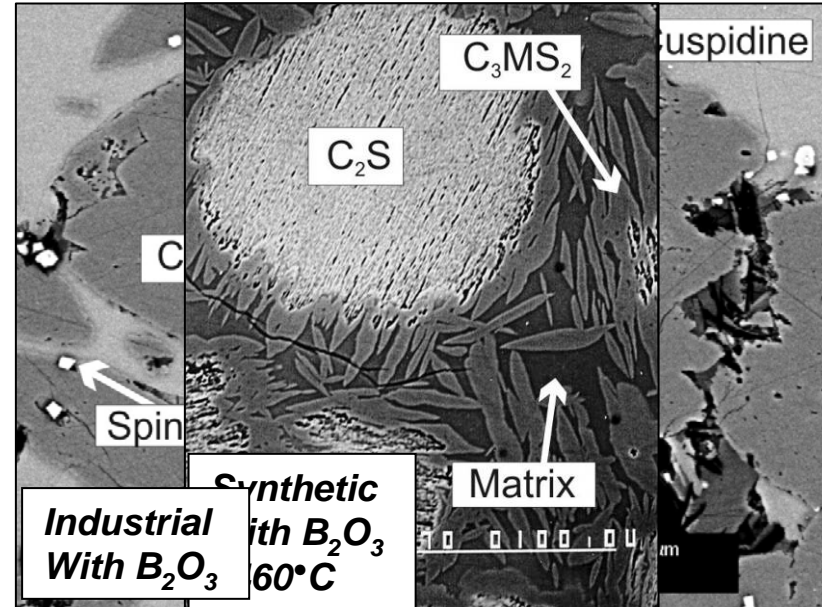
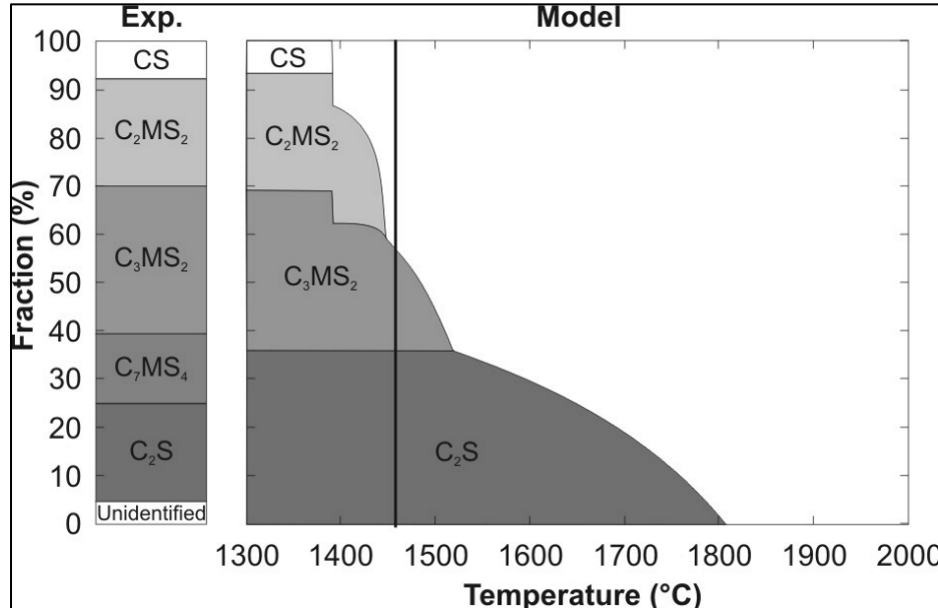


$$L + M + C_2S \rightarrow C_3MS_2$$

Scheil-Gulliver

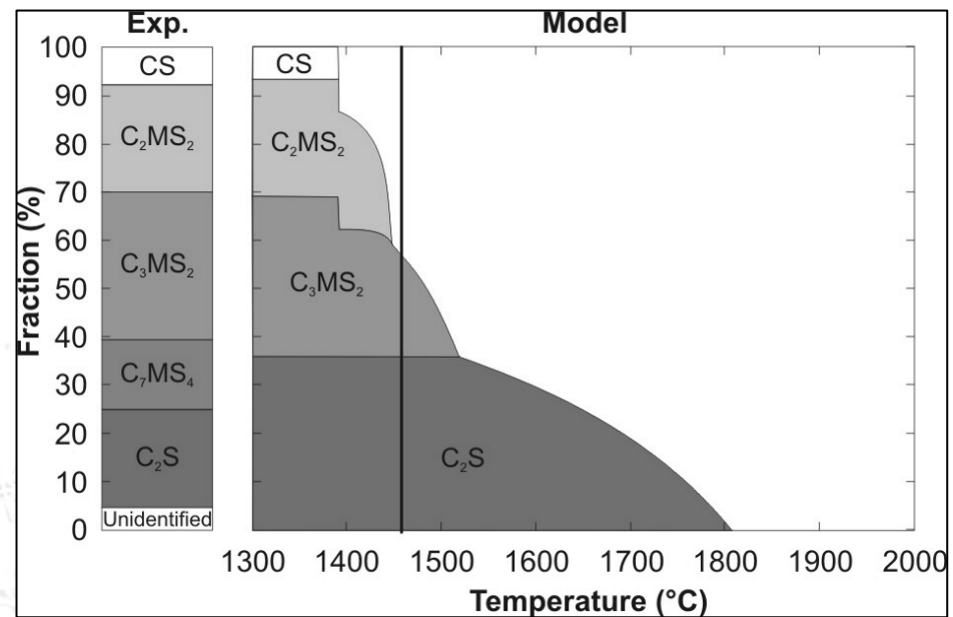
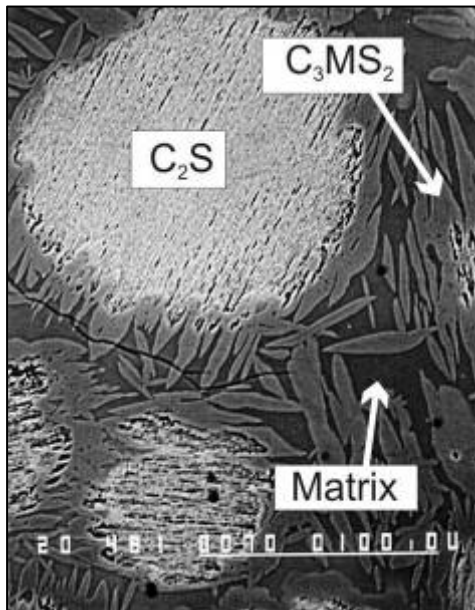


Microstructure



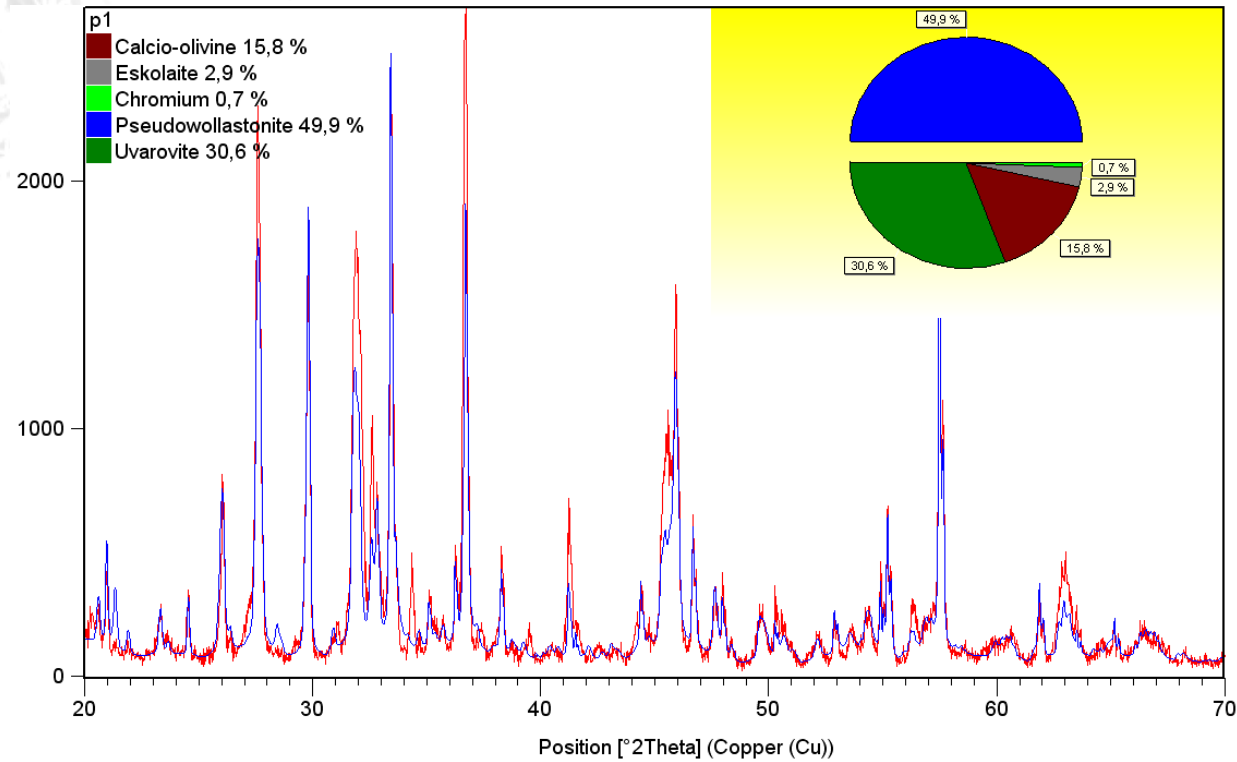
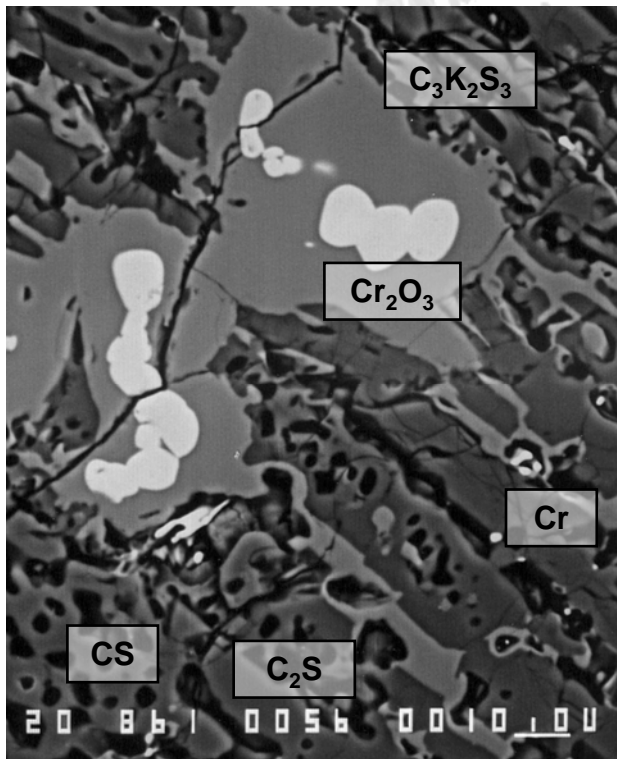
Air-cooled solidification

- pO_2 independent systems (*i.e.* $\text{CaO}-\text{MgO}-\text{SiO}_2$)
 - Scheil-solidification model
 - Lab experiments + QXRD
 - Validated with industrial samples



Air-cooled solidification

□ Preliminary results



Microstructural calculations

- CaO-SiO₂-MgO-CrO_x model system – pO₂ dependent
 - D. Durinck et al., J. Am. Cer. Soc., accepted
- Description of the formation of freeze lining systems
 - Cooperation with E. Jak and P. Hayes
 - M. Campforts et al., Met. Trans. B. , 38B(2007)6, p.841-851
- Phase field modelling for the solidification of oxide systems
 - Cooperation with GTT and Access
 - J. Heulens and N. Moelans

Conclusions

- Basic research tools in high temperature metallurgical research
 - Thermodynamic modeling (ChemApp and FactSage)
 - Process modelling
 - Microstructure calculations
 - Laboratory and industrial experiments
 - Microstructural and (micro-)analytical characterization